Comparison of γ-Aminobutyric Acid, Type A (GABA$_A$), Receptor $\alpha\beta\gamma$ and $\alpha\beta\delta$ Expression Using Flow Cytometry and Electrophysiology

EVIDENCE FOR ALTERNATIVE SUBUNIT STOICHIOMETRIES AND ARRANGEMENTS*

Emmanuel J. Botzolakis[‡1], Katharine N. Gurba[‡1], Andre H. Lagrange[§¶‖1], Hua-Jun Feng[§], Aleksandar K. Stanic[**], Ningning Hu[§], and Robert L. Macdonald[§¶‡‡2]

From the ‡Medical Scientist Training Program and the Departments of §Neurology, ¶Pharmacology, and ‡‡Molecular Physiology and Biophysics, Vanderbilt University, Nashville, Tennessee 37240-7915, the ‖Veterans Affairs Tennessee Valley Healthcare System, Nashville, Tennessee 37212, and the **Department of Obstetrics and Gynecology, University of Wisconsin, Madison, Wisconsin 53792

The subunit stoichiometry and arrangement of synaptic $\alpha\beta\gamma$ GABA$_A$ receptors are generally accepted as $2\alpha{:}2\beta{:}1\gamma$ with a β-α-γ-β-α counterclockwise configuration, respectively. Whether extrasynaptic $\alpha\beta\delta$ receptors adopt the analogous β-α-δ-β-α subunit configuration remains controversial. Using flow cytometry, we evaluated expression levels of human recombinant $\gamma2$ and δ subunits when co-transfected with $\alpha1$ and/or $\beta2$ subunits in HEK293T cells. Nearly identical patterns of $\gamma2$ and δ subunit expression were observed as follows: both required co-transfection with $\alpha1$ and $\beta2$ subunits for maximal expression; both were incorporated into receptors primarily at the expense of $\beta2$ subunits; and both yielded similar FRET profiles when probed for subunit adjacency, suggesting similar underlying subunit arrangements. However, because of a slower rate of δ subunit degradation, 10-fold less δ subunit cDNA was required to recapitulate $\gamma2$ subunit expression patterns and to eliminate the functional signature of $\alpha1\beta2$ receptors. Interestingly, titrating $\gamma2$ or δ subunit cDNA levels progressively altered GABA-evoked currents, revealing more than one kinetic profile for both $\alpha\beta\gamma$ and $\alpha\beta\delta$ receptors. This raised the possibility of alternative receptor isoforms, a hypothesis confirmed using concatameric constructs for $\alpha\beta\gamma$ receptors. Taken together, our results suggest a limited cohort of alternative subunit arrangements in addition to canonical β-α-γ/δ-β-α receptors, including β-α-γ/δ-α-α receptors at lower levels of $\gamma2/\delta$ expression and β-α-γ/δ-α-γ/δ receptors at higher levels of expression. These findings provide important insight into the role of GABA$_A$ receptor subunit under- or overexpression in disease states such as genetic epilepsies.

GABA$_A$ receptors are ligand-gated chloride channels that mediate fast inhibitory neurotransmission. Receptors are assembled as heteropentamers from a large family of subunit subtypes ($\alpha1$–6, $\beta1$–3, $\gamma1$–3, δ, ϵ, θ, π, and $\rho1$–3), with subunit composition determining channel kinetic properties, pharmacological properties, and subcellular localization. For example, although $\alpha\beta\gamma$ receptors are localized to synapses where they produce large extensively desensitizing currents, $\alpha\beta\delta$ receptors are localized to peri- and extrasynaptic compartments where they produce small, slowly desensitizing currents (1–4).

It is generally accepted that $\alpha\beta\gamma$ receptors are composed of two α subunits, two β subunits, and one γ subunit, with a β-α-β-α-γ arrangement (counterclockwise when viewed from the presynaptic terminus) (5–7). The β-α-β-α portion of the pentamer is generally thought to be conserved within ternary receptors, whereas the γ subunit position is thought to be modular, being replaced by other subunit subtypes. For $\alpha\beta\delta$ receptors, support for an analogous stoichiometry of $2\alpha{:}2\beta{:}1\delta$ has been provided by atomic force microscopy (8), site-directed mutagenesis (9), and pharmacological studies (10), with a subunit arrangement of β-α-β-α-δ having been proposed in one study (8). However, alternative receptor stoichiometries and arrangements have been proposed in other studies, not only for $\alpha\beta\delta$ receptors (11–13) but also for $\alpha\beta$ (14, 15), $\alpha\beta\gamma$ (16–20), and $\alpha\beta\epsilon$ receptors (21).

The lack of consensus regarding GABA$_A$ receptor subunit stoichiometry and arrangement likely reflects the highly variable methodologies employed to date. For example, although some studies have evaluated receptors composed of "freely assembled" subunits, others have utilized receptors assembled from concatenated subunits (5, 14). Concatenation is unquestionably a powerful experimental approach, often representing the only way to definitively test whether a particular subunit arrangement is functional. However, the results represent forced subunit assembly and therefore must not be interpreted in isolation. Concatenation may reveal what subunit stoichiometries and arrangements are theoretically possible, but whether the receptors adopt these configurations naturally is another matter. Moreover, concatenation has known technical limitations, requiring that extensive control experiments be performed to exclude the possibility of "looped out" subunits or

[1] These authors contributed equally to this work.

[2] To whom correspondence should be addressed: Vanderbilt University Medical Center, 6140 Medical Research Bldg. III, 465 21st Ave. South, Nashville, TN 37240-7915. Tel.: 615-936-2287; Fax: 615-322-5517; E-mail: robert.macdonald@vanderbilt.edu.

linker sequence cleavage (22, 23). Expression systems also commonly differ between studies, with some having used human-derived cell lines, but many others having used *Xenopus* oocytes to boost protein expression. Additional differences in experimental methodology have included the species of subunits employed (*e.g.* rat *versus* human) and the identity of partnering subunits (*e.g.* β2 *versus* β3), which could theoretically affect receptor composition.

To improve our understanding of GABA$_A$ receptor biogenesis, we compared the surface and total cellular expression profiles of human γ2 and δ subunits permitted to freely assemble with α1 and β2 subunits in HEK293T cells using a multimodality approach that included flow cytometry, whole cell patch clamp recording (using both freely assembled and concatenated subunits), and traditional biochemistry techniques. By combining these methodologies, we deduced that αβγ and αβδ receptors have similar stoichiometries and arrangements. However, 10-fold lower concentrations of δ subunit cDNA were required to recapitulate γ2 subunit expression profiles, reflecting a slower rate of δ subunit degradation. Moreover, we found that αβγ and αβδ receptor composition depends on relative subunit availability, with alternative subunit arrangements and stoichiometries likely occurring with increasing levels of γ or δ subunit expression.

Results

GABA$_A$ Receptor γ2L^{HA} and δ^{HA} Subunits Had Different Profiles of Surface Expression When Co-transfected with α1 and/or β2 Subunits at Equimolar cDNA Ratios—To determine the subunit requirements for receptor surface trafficking, we transfected HEK293T cells with all possible combinations of α1, β2, γ2L, and δ subunit cDNAs (excluding conditions with γ2L and δ subunit co-transfection), labeled subunits with fluorescently conjugated antibodies, and evaluated cell surface fluorescence levels using flow cytometry. Although there has been ongoing debate in the GABA$_A$ receptor literature regarding what subunit cDNA ratios should be transfected in recombinant receptor studies (27–29), we chose to begin with equimolar ratios because this should approximate the relative gene dosage *in vivo* (α1, β2, γ2, and δ GABA$_A$ receptor subunit genes are autosomal and none has been shown to be imprinted). Because no commercially available antibodies against γ2 or δ subunits were found to be suitable for flow cytometry (secondary to excessive nonspecific binding), the HA epitope (YPYDVPDYA) was inserted near the N termini of γ2L and δ subunits (see under "Experimental Procedures"), and levels of these subunits were detected using a fluorescently conjugated anti-HA antibody.

Of note, there were two primary reasons for using HEK293T cells as opposed to neurons or neuronal cell lines in these experiments. Most importantly, HEK293T cells have minimal if any endogenous expression of GABA$_A$ receptor subunits, the presence of which could confound conclusions reached about receptor assembly. Although a few studies have reported low levels of endogenous β3 subunit expression in HEK293 cells, this has not been a consistent finding in the literature (30–32), and it has never been confirmed in our laboratory despite extensive investigation (data not shown). In contrast, neurons

are known to express high and variable levels of multiple endogenous GABA$_A$ receptor subunits. HEK293T cells are also ideal subjects for flow cytometry experiments, as they are easily harvested and express reproducible levels of subunit protein. In contrast, harvesting of neurons typically results in loss of neuronal processes and, consequently, loss of many postsynaptic GABA$_A$ receptors.

Our results demonstrate that α1 (Fig. 1, *A* and *D*) and β2 (Fig. 1, *B* and *E*) subunits were efficiently trafficked to the cell surface when co-expressed but not when transfected alone, excluding the possibility of significant endogenous expression of either subunit. Very low levels of α1 subunit surface expression were detected in all α1 subunit-containing transfection conditions lacking the β2 subunit, noting that the levels of the α1 subunit were not significantly affected by co-expression with γ2L^{HA} or δ^{HA} subunits (α1 = 2.9 ± 0.3%, α1γ2L^{HA} = 5.2 ± 0.2%, and α1δ^{HA} = 3.1 ± 0.5% of α1β2; n = 6). The β2 subunit was not detected on the cell surface when transfected either alone or in combination with γ2L^{HA} or δ^{HA} subunits. Consistent with previous studies (24, 33), γ2L^{HA} subunits reached the cell surface at low levels when transfected alone or in combination with α1 or β2 subunits, but they were maximally expressed on the cell surface only when co-expressed with α1 and β2 subunits (Fig. 1, *C* and *F*) (γ2L^{HA} = 6.5 ± 0.9%, α1γ2L^{HA} = 9.6 ± 1.6%, and β2γ2L^{HA} = 8.9 ± 0.7 of α1β2γ2L^{HA}; n = 6). In contrast, δ^{HA} subunits reached the cell surface even when transfected alone, and surface expression levels were not significantly affected by co-transfection with α1 and/or β2 subunits (Fig. 1, *C* and *F*) (δ^{HA} = 26.1 ± 6.3%, α1δ^{HA} = 37.0 ± 9.8%, β2δ^{HA} = 26.7 ± 5.6%, and α1β2δ^{HA} = 39.8 ± 8.1% of α1β2γ2L^{HA}; n = 6).

Perhaps the most unexpected results involved the equimolar α1β2γ2L^{HA} and α1β2δ^{HA} subunit co-transfection conditions. Although αβγ and αβδ GABA$_A$ receptor isoforms are known to differ greatly in their physiological and pharmacological properties (1), the receptors are generally thought to have similar ternary structure (34). Therefore, it was surprising that α1 subunit surface levels with α1β2γ2L^{HA} subunit co-expression were ~90% of those with α1β2 subunit co-expression (93.0 ± 4.0% of α1β2; n = 6), whereas α1 subunit surface levels with α1β2δ^{HA} subunit co-expression were only ~10% of those with α1β2 co-expression (10.6 ± 0.4% of α1β2; n = 6) (Fig. 1, *A* and *D*). A difference was also seen in the surface expression patterns of the β2 subunit (Fig. 1, *B* and *E*), which decreased to ~30% of α1β2 levels following addition of the γ2L^{HA} subunit (31.6 ± 1.3% of α1β2; n = 5) but decreased to only ~5% of α1β2 levels following addition of the δ^{HA} subunit (6.2 ± 1.3% of α1β2; n = 5).

GABA$_A$ Receptor γ2L^{HA} and δ^{HA} Subunits Had Different Profiles of Total Cellular Expression When Co-transfected with α1 and/or β2 Subunits at Equimolar cDNA Ratios—The results in the previous section demonstrated that α1 and β2 subunit surface expression levels were differentially affected by co-transfection with an equimolar ratio of γ2L^{HA} or δ^{HA} subunit cDNA. To explore whether the different patterns of subunit surface expression reflected differential subunit surface trafficking, differential subunit expression, or perhaps a combination of both, total cellular expression levels were assessed by repeating the previously described flow cytometry experiments following cell
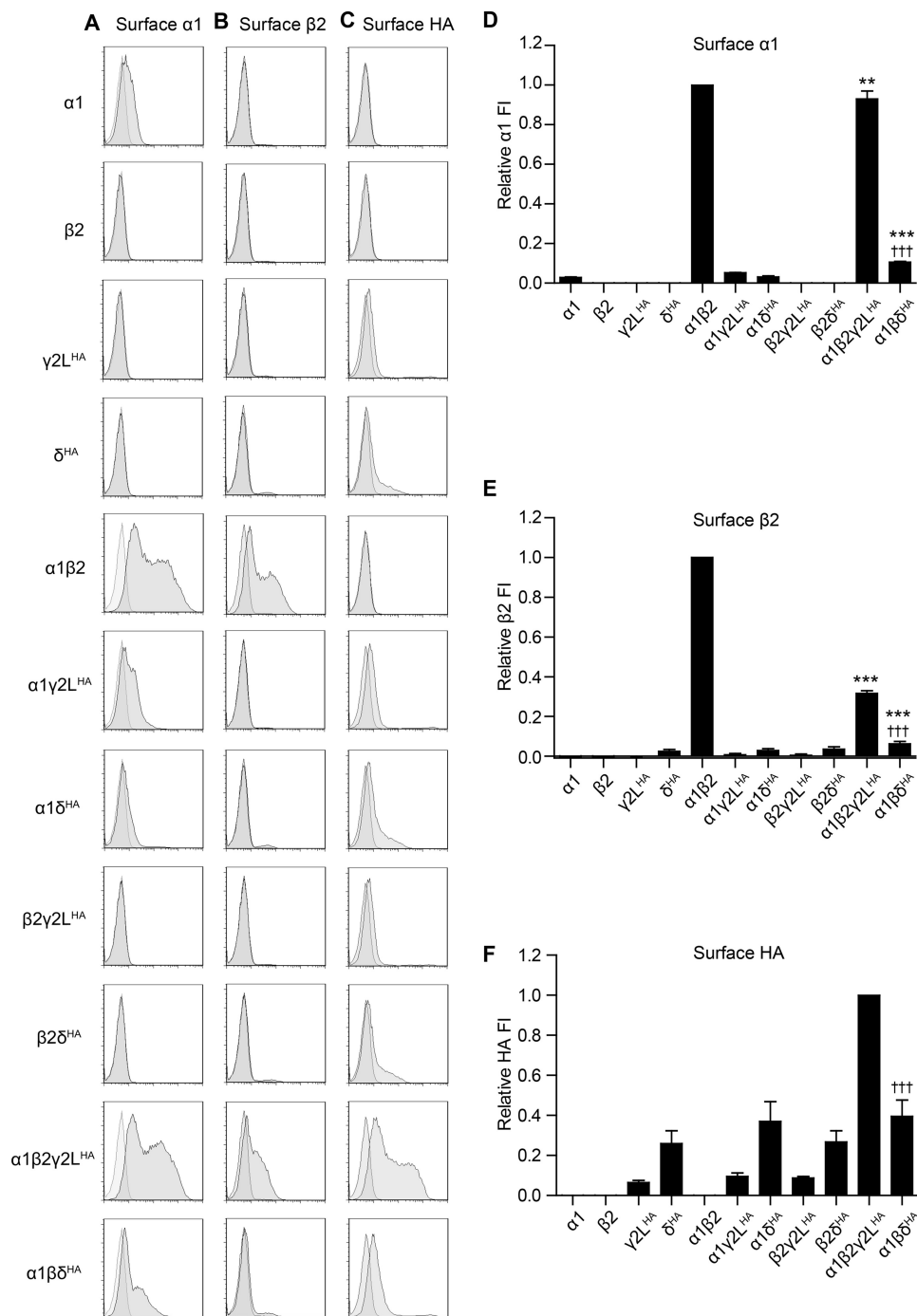
FIGURE 1. **GABA_A receptor α1, β2, γ2L^HA, and δ^HA subunit surface expression was highly sensitive to the presence and identity of partnering subunits.** HEK293T cells were transfected with various combinations of GABA_A receptor subunit cDNAs, and surface expression was evaluated using subunit-specific antibodies and flow cytometry. *A–C* present representative flow cytometry histograms from cells transfected with the indicated combination of subunit cDNAs (*left*) and incubated with antibodies raised against α1 (*A*), β2/3 (*B*), GABA_A receptor subunits or the HA epitope tag (*C*). The *abscissa* indicates fluorescence intensity (*FI*) in arbitrary units plotted on a logarithmic scale, and the *ordinate* indicates percentage of maximum cell count (% of maximum). *Histograms* for cells transfected with subunit combinations (*dark gray*) and cells transfected with blank vector (*light gray*) are overlaid. *D–F* present quantifications of fluorescence intensities from cells transfected with the indicated combination of subunit cDNAs and incubated with antibodies raised against α1 (*D*) or β2/3 (*E*) GABA_A receptor subunits or the HA epitope tag (*F*). Mean fluorescence intensities from cells transfected with blank vector alone were subtracted from mean fluorescence intensities of all other expression conditions. All mock-subtracted fluorescence intensities were normalized to the mock-subtracted fluorescence intensity obtained with α1β2γ2L^HA subunit co-expression. **, $p < 0.01$; ***, $p < 0.001$ *versus* α:β and †††, $p < 0.001$ *versus* α:β:γ2L.

membrane permeabilization (Fig. 2). Of note, monitoring total expression levels also served as an important control for the flow cytometry assay, as it confirmed that the monoclonal antibodies being used to detect GABA_A receptor subunits were highly specific for their respective subunits or epitopes. The α1

subunit antibody, for example, was detected intracellularly in all transfection conditions that included α1 subunit cDNA but none that lacked α1 subunit cDNA (Fig. 2A). The same was also true for the β2 subunit and HA epitope antibodies (Fig. 2, *B* and *C*).
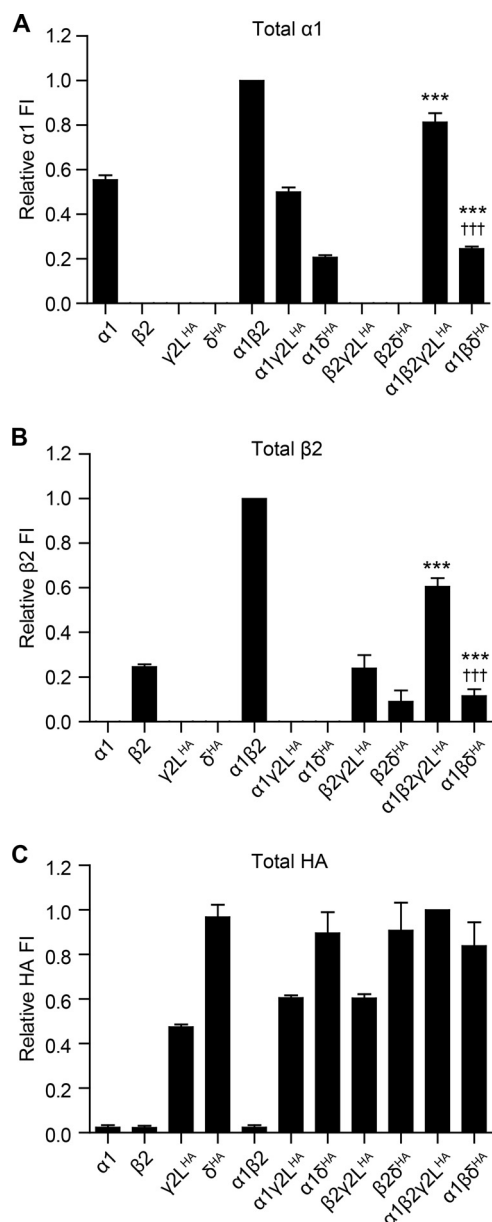
FIGURE 2. GABA$_A$ receptor $\alpha1$, $\beta2$, $\gamma2L^{HA}$, and δ^{HA} subunit total cellular expression was highly sensitive to the presence and identity of partnering subunits. HEK293T cells were transfected with various combinations of GABA$_A$ receptor subunit cDNAs, and total cellular subunit expression was evaluated after cell membrane permeabilization using flow cytometry. *A–C*, fluorescence intensities were quantified from cells transfected with the indicated combination of subunit cDNAs and incubated with antibodies raised against $\alpha1$ (*A*) or $\beta2/3$ (*B*) GABA$_A$ receptor subunits or the HA epitope tag (*C*). Mean fluorescence intensities from cells transfected with blank vector alone were subtracted from mean fluorescence intensities of all other expression conditions. All mock-subtracted fluorescence intensities were normalized to the mock-subtracted fluorescence intensity obtained with $\alpha1\beta2\gamma2L^{HA}$ subunit co-expression. , ***, $p < 0.001$ *versus* $\alpha:\beta$ and †††, $p < 0.001$ *versus* $\alpha:\beta:\gamma2L$.

Although there was only minimal $\alpha1$ subunit surface expression when transfected alone or in the presence of either $\gamma2L^{HA}$ or δ^{HA} subunits (Fig. 1), moderate levels of the $\alpha1$ subunit were detected in these conditions following membrane permeabilization (Fig. 2*A*) ($\alpha1 = 55.3 \pm 2.2\%$, $\alpha1\gamma2L^{HA} = 50.0 \pm 2.1\%$, and $\alpha1\delta^{HA} = 20.6 \pm 1.1\%$ of $\alpha1\beta2$; $n = 6$), indicating that $\alpha1$ subunits were predominantly trapped intracel-

lularly in the absence of $\beta2$ subunits. Similar findings were obtained with the $\beta2$ subunit, which had no detectable surface expression when transfected alone or in the presence of $\gamma2L^{HA}$ or δ^{HA} subunits but was identified at low levels in these conditions following membrane permeabilization (Fig. 2*B*) ($\beta2 = 24.7 \pm 1.2\%$, $\beta2\gamma2L^{HA} = 24.0 \pm 5.9\%$, and $\beta2\delta^{HA} = 9.0 \pm 5.1\%$ of $\alpha1\beta2$; $n = 5$), indicating that $\beta2$ subunits were trapped intracellularly unless co-transfected with $\alpha1$ subunits. The same was also true of the $\gamma2L^{HA}$ subunit, which had low levels of surface expression when transfected alone or in the presence of either or $\alpha1$ or $\beta2$ subunits but had moderate levels of total cellular expression in these conditions (Fig. 2*C*) ($\gamma2L^{HA} = 46.2 \pm 1.4\%$, $\alpha1\gamma2L^{HA} = 59.6 \pm 1.0\%$, $\beta2\gamma2L^{HA} = 59.6 \pm 1.8\%$ of $\alpha1\beta2\gamma2L^{HA}$; $n = 5$). The only subunit that did not follow this pattern was the δ^{HA} subunit, which demonstrated high levels of both surface and total cellular expression when transfected alone as well as with all other subunit combinations (Fig. 2*C*) ($\delta^{HA} = 96.9 \pm 5.6\%$, $\alpha1\delta^{HA}$ $89.5 \pm 5.0\%$, $\beta2\delta^{HA} = 91.2 \pm 12.6\%$, and $\alpha1\beta2\delta^{HA} = 83.7 \pm 10.6\%$ of $\alpha1\beta2\gamma2L^{HA}$; $n = 6$).

In the setting of ternary $\alpha1\beta2\gamma2L^{HA}$ and $\alpha1\beta2\delta^{HA}$ subunit transfection, the patterns of total cellular expression more closely resembled those of surface subunit expression, likely indicating that a substantial fraction of the total subunit pool was present on the cell surface. For instance, $\alpha1$ subunit total expression levels were ~80% of $\alpha1\beta2$ levels when the $\gamma2L^{HA}$ subunit was co-transfected ($\alpha1\beta2\gamma2L^{HA} = 81.3 \pm 4.1\%$ of $\alpha1\beta2$; $p < 0.01$) and ~25% of $\alpha1\beta2$ levels when the δ^{HA} subunit was co-transfected ($\alpha1\beta2\delta^{HA} = 24.5 \pm 1.0\%$ of $\alpha1\beta2$; $p < 0.001$ compared with both $\alpha1\beta2$ and $\alpha1\beta2\gamma2L^{HA}$). Total cellular expression of $\beta2$ subunits also mirrored the patterns seen with surface expression decreasing by almost half compared with $\alpha1\beta2$ levels when $\gamma2L^{HA}$ subunits were included ($\alpha1\beta2\gamma2L^{HA} = 60.5 \pm 3.9\%$ of $\alpha1\beta2$; $p < 0.001$) and to ~10% of $\alpha1\beta2$ levels when δ^{HA} subunits were included ($\alpha1\beta2\delta^{HA} = 11.6 \pm 3.1\%$ of $\alpha1\beta2$; $p < 0.001$ compared with both $\alpha1\beta2$ and $\alpha1\beta2\gamma2L^{HA}$).

By comparing the patterns of surface and total cellular expression, several conclusions could be drawn. First, it appeared that co-expression of $\alpha1$ and $\beta2$ subunits was both necessary and sufficient for surface trafficking of all tested subunits except for the δ^{HA} subunit, which was trafficked to the cell surface independent of subunit combination. Second, in contrast to $\gamma2L^{HA}$ subunits, co-transfection of δ^{HA} subunits resulted in a marked decrease in both surface and total cellular expression levels of partnering subunits independent of transfection condition, suggestive of a potent dominant negative effect. Although the basis for this dominant negative effect is uncertain based on the results of these experiments alone, it should be noted that δ^{HA} subunit co-transfection even decreased total cellular expression of the $\beta2$ subunit, which could not reach the cell surface when transfected alone. This suggests that the dominant negative effects of the δ^{HA} subunit were, at least in part, mediated by promoting subunit degradation. Third, given that surface and total cellular expression levels of the δ^{HA} subunit were essentially constant across transfection conditions (Figs. 1 and 2) and not significantly different compared with expression levels of the δ^{HA} subunit transfected alone (despite universally decreased expression levels of partnering subunits), it seems likely that the majority of δ^{HA} sub-

units trafficked to the cell surface were unassembled with co-transfected subunits.

Decreasing the Amount of δ^{HA} Subunit cDNA Co-transfected with α1 and β2 Subunits by 10-Fold Recapitulated γ2L^{HA} Subunit Surface Expression Patterns—Up to this point, the results of surface and total cellular expression studies raised the possibility that γ2L and δ subunits were incorporated into ternary GABA_A receptors quite differently. However, one important similarity could not be ignored; addition of both γ2L and δ subunits had disparate effects on α1 and β2 surface and total expression levels. Despite the profound dominant negative effect of adding the δ subunit on partnering subunit expression, β2 subunit expression levels were consistently more reduced than α1 levels, a phenomenon also observed for the γ2L subunit. We therefore hypothesized that differences observed between γ2L and δ subunits simply reflected differences in subunit "availability," as opposed to intrinsic differences in receptor stoichiometry and/or arrangement. Indeed, the relatively constant patterns of surface and total cellular expression observed with δ subunit co-transfection (independent of subunit combination) could be a manifestation of marked protein overexpression, which can overload normal cellular trafficking machinery, activate protein degradation pathways, and trigger apoptosis. Consistent with the latter, we noted considerably higher rates of cell death in all conditions involving 1 μg of δ subunit transfection, but not γ2L transfection, unless the latter was transfected in considerable excess (10 μg; data not shown).

To explore this possibility, surface and total cellular expression levels were again evaluated with flow cytometry but with variable amounts of γ2L^{HA} or δ^{HA} cDNA transfected (Fig. 3). Specifically, the amount of α1 and β2 subunit cDNA transfected was held constant (1 μg per subunit), although the amount of γ2L^{HA} or δ^{HA} cDNA was systematically increased over several orders of magnitude. Of note, evaluation of subunit expression was not possible when more than 1 μg of δ^{HA} cDNA was transfected, as this resulted in widespread cell death. The results demonstrated that increasing the amount of γ2L^{HA} or δ^{HA} subunit cDNA transfected yielded similar overall patterns of subunit expression but with far less δ^{HA} subunit cDNA being required to produce comparable expression levels (*i.e.* the δ^{HA} subunit cDNA titration curves were all left-shifted compared with those of the γ2L^{HA} subunit). For instance, α1 subunit surface levels remained relatively stable when low levels of γ2L^{HA} subunit cDNA were transfected (Fig. 3A) and began progressively decreasing only after >0.3 μg of γ2L^{HA} subunit cDNA was transfected (Fig. 3A, *black line*). A similar "plateau" phase was seen with increasing δ^{HA} subunit cDNA levels; however, the subsequent progressive decrease began when the δ^{HA} subunit cDNA level was only ≥0.03 μg (Fig. 3A, *gray line*). Surface expression levels of the β2 subunit also responded similarly to increasing amounts of γ2L^{HA} or δ^{HA} cDNA transfected, but again with far less δ^{HA} subunit cDNA required to produce comparable expression levels. The pattern, however, was distinct from that seen with the α1 subunit. Instead of an early plateau phase, increasing amounts of γ2L^{HA} or δ^{HA} subunit cDNA caused steady concentration-dependent decreases in β2 subunit surface levels (Fig. 3B), suggestive of γ2L^{HA} or δ^{HA} subunit incorporation into ternary subunits occurring primarily at the

expense of β2 subunits. Finally, γ2L^{HA} and δ^{HA} subunit surface levels also had similar patterns with increasing cDNA levels, but with the δ^{HA} curve again appearing left-shifted compared with the γ2L^{HA} curve. For both subunits, surface levels increased over a range of cDNA levels, peaked, and then decreased (Fig. 3C). However, peak subunit surface expression occurred with only 0.03 μg of δ^{HA} cDNA, as compared with 1 μg of γ2L^{HA} cDNA. Notably, peak γ2L^{HA} and δ^{HA} subunit surface levels were not achieved until after α1 subunit surface levels began to decline, suggesting that at higher transfection ratios, incorporation of γ2L^{HA} and δ^{HA} subunits into ternary receptors could also occur at the expense of α1 subunits. Of note, although the highest transfection ratios for the γ2L^{HA} subunit (1:1:3 and 1:1:10) included higher amounts of γ2L^{HA} subunit cDNA than other transfection conditions (5 and 12 μg, respectively; see "Experimental Procedures"), the overall patterns of α1, β2, and γ2L^{HA} subunit surface and total cellular expression were similar to those obtained at the highest levels of δ^{HA} subunit expression, where total cDNA levels were maintained at 3 μg.

Total cellular subunit expression patterns over a range of γ2L^{HA} and δ^{HA} subunit cDNA levels were generally similar to surface expression patterns, noting that total cellular subunit protein levels decreased to a lesser extent at the highest amounts of γ2L^{HA} or δ^{HA} cDNA. Levels of α1 subunits began declining when more than 0.3 μg of γ2L^{HA} subunit cDNA or 0.01 μg of δ^{HA} subunit cDNA was transfected (Fig. 3D), whereas levels of β2 subunits began declining when more than 0.01 μg of either γ2L^{HA} or δ^{HA} subunit cDNA was transfected (Fig. 3E). Interestingly, the total cellular expression patterns of γ2L^{HA} and δ^{HA} subunits were somewhat different from their surface expression patterns (Fig. 3F). Here, γ2L^{HA} subunit levels peaked when 3 μg (as opposed to 1 μg) of cDNA was transfected, after which they declined from that peak by ~25% with 10 μg of cDNA transfected (as opposed to the 80% decrease in surface expression). Similarly, although δ^{HA} subunit surface levels peaked when 0.03 μg of cDNA was transfected and declined by about 75% when 1 μg of cDNA was transfected, δ^{HA} total cellular levels steadily increased over the entire range of cDNA amounts.

These findings supported several conclusions. First and foremost, the observation that increasing amounts of γ2L^{HA} and δ^{HA} subunit cDNA had nearly identical effects on the expression profiles of partnering subunits argues against significant differences in how these subunits were incorporated into ternary receptors. Both γ2L^{HA} and δ^{HA} subunits appeared on the cell surface at the expense of β2 subunits, noting a range of γ2L^{HA}/δ^{HA} subunit cDNA amounts over which α1 subunit levels did not change, β2 subunit levels decreased, and γ2L^{HA}/δ^{HA} subunit levels increased. At higher transfection ratios, both γ2L^{HA} and δ^{HA} subunit surface expression levels continued to rise sharply despite concomitant decreases in both α1 and β2 subunit levels, suggesting that incorporation into ternary receptors could also occur at the expense of α1 subunits when sufficient competing γ2L^{HA} or δ^{HA} subunit was available. In addition, both γ2L^{HA} and δ^{HA} subunits appeared to require co-transfection with α1 and β2 subunits for maximal surface expression, as surface levels were considerably lower at all titra-
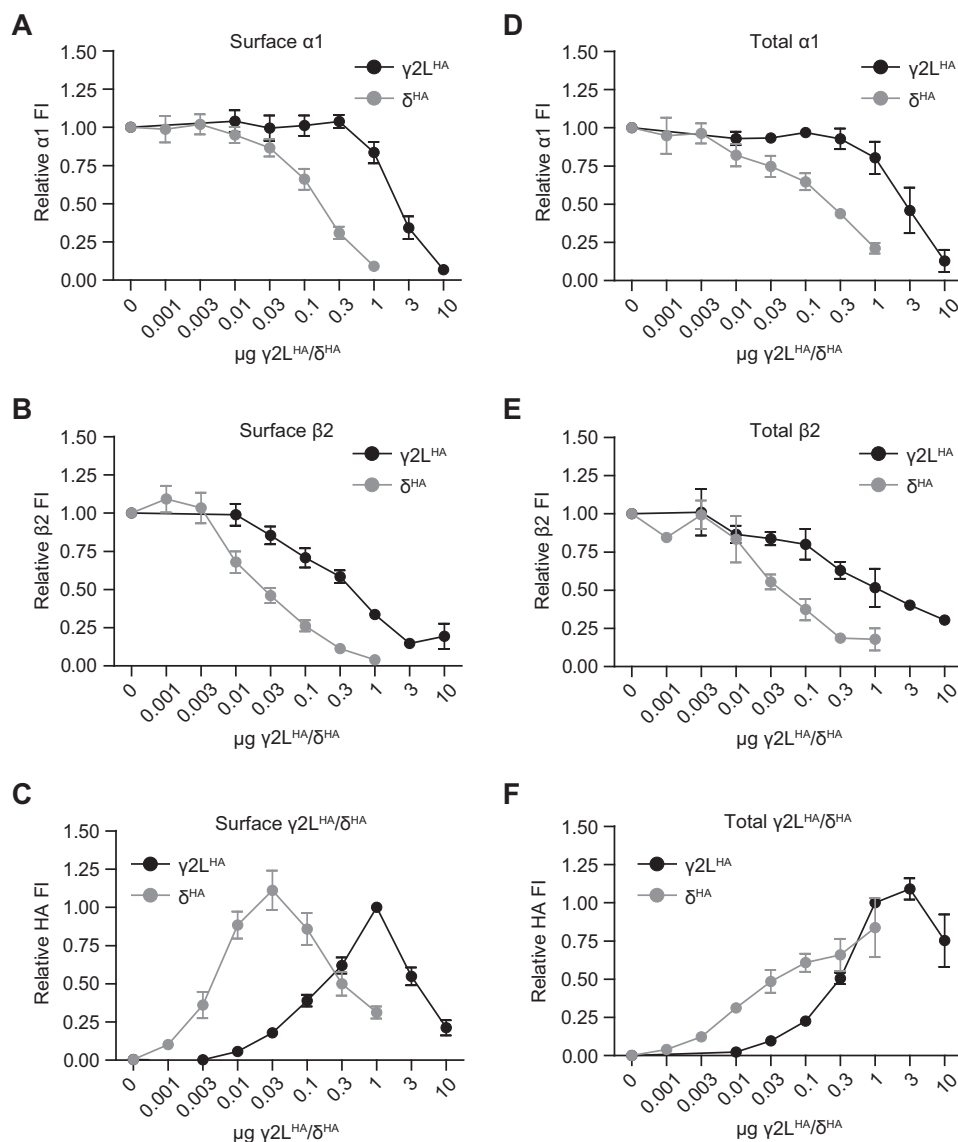
FIGURE 3. **GABA_A receptor α1, β2, and γ2L^HA or δ^HA subunits had similar surface and total expression levels and patterns but required markedly different amounts of γ2L^HA or δ^HA cDNA.** Flow cytometry was used to evaluate surface and total expression of GABA_A receptor subunits in HEK293T cells transfected with α1, β2, and varying amounts of γ2L^HA or δ^HA subunit cDNAs. *A–C,* surface expression levels of α1 (*A*), β2 (*B*), and γ2L^HA (*C*) subunits were evaluated in cells transfected with 1 μg of α1 subunit cDNA, 1 μg of β2 subunit cDNA, and 0.01–10 μg of γ2L^HA subunit cDNA. Mean fluorescence intensities from cells transfected with blank vector alone were subtracted from mean fluorescence intensities of all other expression conditions. All mock-subtracted fluorescence intensities were normalized to the mock-subtracted fluorescence intensity obtained with 1 μg of α1, 1 μg of β2, 1 μg of γ2L^HA subunit co-expression. *D–F,* total expression levels of α1 (*D*), β2 (*E*), and γ2L^HA (*F*) subunits were evaluated in cells transfected with 1 μg of α1 subunit cDNA, 1 μg of β2 subunit cDNA, and 0.001–1 μg of δ^HA subunit cDNA. Mean fluorescence intensities from cells transfected with blank vector alone were subtracted from mean fluorescence intensities of all other expression conditions. All mock-subtracted fluorescence intensities were normalized to the mock-subtracted fluorescence intensity obtained with 1 μg of α1, 1 μg of β2, 0.1 μg of δ^HA subunit co-expression.

tion points when γ2L^HA and δ^HA subunits were transfected alone (data not shown). Finally, both γ2L^HA and δ^HA subunits appeared capable of exerting a profound dominant negative effect on co-transfected subunit levels at the highest transfection ratios, as surface levels of all subunits declined after γ2L^HA/δ^HA subunit levels peaked, after which there was also considerable cell death not seen in cells treated with equivalent levels of transfection reagent and blank pcDNA vector (data not shown).

Fluorescence Resonance Energy Transfer (FRET) Analysis Suggested Similar Patterns of Subunit Adjacency in α1β2γ2L and α1β2δ Containing Receptors—FRET is an established methodology for monitoring protein-protein interactions (35). In contrast to conventional biochemical techniques (*e.g.* co-

immunoprecipitation), FRET can be used to monitor proteins in their native conformations and to identify direct protein interactions. Although FRET can be measured by spectrofluorimetry and microscopy, flow cytometry offers several advantages over these techniques. Unlike spectrofluorimetry, measurements can be performed on individual cells, and importantly, donor emission can easily be distinguished from sensitized emission of the acceptor. Although microscopy allows the subcellular localization of protein interactions to be evaluated, the technique is less sensitive, analysis is labor-intensive and poorly quantitative, and selecting regions of interest is highly subjective. Flow cytometry, in contrast, allows for rapid, quantitative, and unbiased analysis of FRET in large cell popu-

lations and permits the simultaneous analysis of other cellular properties (*e.g.* viability) (36).

Based on homology modeling to nAChRs, GABA$_A$ receptors are thought to assemble into pseudo-symmetrical pentamers (37). As a result, each subunit is predicted to have two "adjacent" subunits and two "non-adjacent" subunits. Given the crystal structure of the homomeric β3 subunit GABA$_A$ receptor (38), the N termini (where our subunit- and epitope-specific antibodies bind) of adjacent subunits in ternary α1β2γ2L and α1β2δ receptors are likely separated by ∼30–40 Å, whereas those of non-adjacent subunits are likely separated by ∼50–60 Å (accounting for slight differences in N-terminal length between subunit subtypes and due to epitope tagging). Because FRET efficiency is inversely proportional to the sixth power of distance (35), adjacent subunits would be expected to yield a more robust FRET signal as compared with non-adjacent subunits. For ternary receptors, there are six possible subunit combinations that can be probed with a FRET assay (*e.g.* for α1β2γ2L receptors, FRET could potentially occur between α1 subunits, between β2 subunits, between γ2L subunits, between α1 and β2 subunits, between α1 and γ2L subunits, and between β2 and γ2L subunits). By analyzing the FRET signals between all possible subunit combinations, a FRET "profile" can be generated for each isoform. If αβγ and αβδ receptors have different subunit stoichiometries and/or arrangements, then distinct FRET profiles would be predicted.

To perform the FRET assay, transfected cells were co-stained with equimolar mixtures of donor-conjugated (Alexa-555) and acceptor-conjugated (Alexa-647) subunit-specific antibodies (Förster radius for this fluorophore pair was 51 Å). The resulting FRET signal was evaluated using flow cytometry, as described previously (39). Specifically, the FRET signal represented emission detected from the acceptor fluorophore following excitation of the donor fluorophore, using an excitation wavelength that could not significantly excite the acceptor fluorophore directly. Of note, the exact distance between donor and acceptor fluorophores in this experimental paradigm was uncertain, as the configuration of antibodies bound to the GABA$_A$ receptor subunits and the location of fluorophores conjugated to the antibodies were unknown. This uncertainty precluded *a priori* estimation of FRET efficiency between these fluorophores.

To determine whether there was a significant contribution of FRET from non-adjacent subunits in this experimental paradigm, concatenated α1-β2 subunits were co-transfected with the β2^{HA} subunit, forcing the β2^{HA}-α1-β2-α1-β2 subunit arrangement. Co-staining this receptor with donor-conjugated anti-HA and acceptor-conjugated anti-α1 antibodies, FRET was detected between the β^{HA} subunit and the concatenated α1 subunit (*n* = 4), confirming FRET between adjacent subunits. In contrast, co-staining with a mixture of donor- and acceptor-conjugated anti-α1 antibodies demonstrated no FRET, indicating that FRET could not occur between non-adjacent subunits. FRET was also not observed when receptors were co-stained with a mixture of donor- and acceptor-conjugated anti-HA antibodies, indicating that FRET could not occur between pentamers (data not shown). However, we cannot exclude the possibility that antibodies bound to freely assembled subunits have
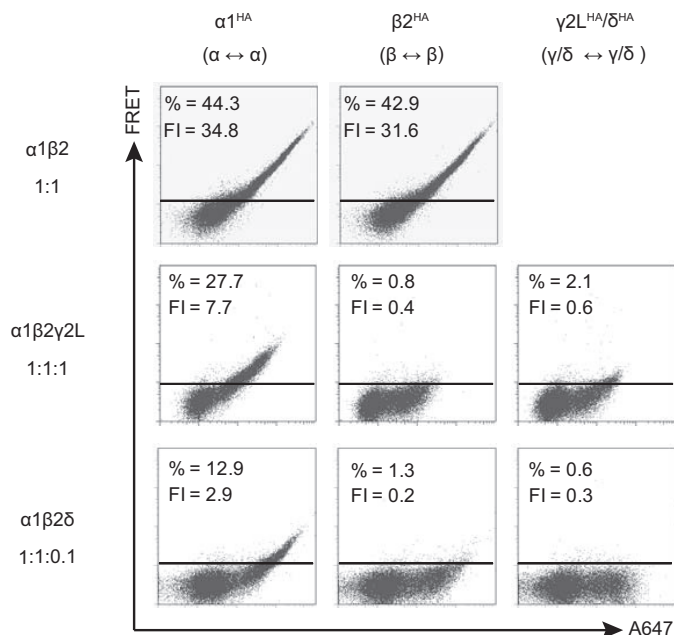

FIGURE 4. **Flow cytometric analysis of GABA$_A$ receptor γ2L^{HA} and δ^{HA} subunit FRET with partnering α1 and β2 subunits when transfected at "expression-equivalent" levels suggested that γ2L^{HA} and δ^{HA} subunits assembled in similar patterns.** HEK293T cells were transfected with 1 μg of α1 subunit cDNA, 1 μg of β2 subunit cDNA, and either blank pcDNA vector or the amount of γ2L^{HA} or δ^{HA} subunit cDNA that achieved maximal expression (Fig. 3). The α1 and β2 subunit cDNAs were co-transfected with 1 μg of pcDNA vector (*top row*), 1 μg of γ2L^{HA} subunit cDNA (*middle row*), or 0.1 μg δ^{HA} cDNA + 0.9 μg of pcDNA vector (*bottom row*). To determine subunit adjacency, each subunit was individually HA-tagged, and cells were incubated with both anti-HA-Alexa-555 and anti-HA-Alexa-647 before being subjected to flow cytometry. The *left column* illustrates the α1-α1 subunit FRET signal (α1 HA-tagged); the *middle column* illustrates the β2-β2 subunit FRET signal (β2 HA-tagged); and the *right column* illustrates the γ2L-γ2L or δ-δ FRET signal. For all dot plots, the *x* axis indicates fluorescence intensity of the acceptor fluorophore (Alexa-647) when excited directly, and the *y* axis (FRET) indicates fluorescence intensity of acceptor fluorophore (Alexa-647) when only the donor fluorophore (Alexa-555) was excited. The *horizontal line* indicates the FRET threshold, defined such that less than 1% of cells are located above this line when stained with only acceptor fluorophore (*i.e.* where FRET was not possible). The percentage of cells emitting above this threshold is listed at the *top* of each dot plot along with the mean FRET fluorescence intensity (*FI*).

slightly different orientations compared with those bound to concatameric subunits, which might permit FRET between non-adjacent subunits. With that said, the primary goal of these experiments was to compare the FRET profiles of αβγ and αβδ receptors, in the hope of exposing differences in their underlying stoichiometries and/or arrangements, and not to explicitly to deduce them.

To determine whether identical subunits could generate a FRET signal in freely assembled α1β2, α1β2γ2L, and α1β2δ receptors, one subunit was HA-tagged at a time per transfection condition (*e.g.* α1^{HA}β2), and the resulting receptors were stained with an equal mixture of HA-A555 (donor) and HA-647 (acceptor) antibodies. For α1β2 receptors (Fig. 4, *top row*), a robust FRET signal was observed between individual α1^{HA} subunits and between individual β2^{HA} subunits with α1β2^{HA} co-transfection (*n* = 4). When α1 and β2 subunits were co-expressed with γ2L (1 μg; Fig. 4, *middle row*; *n* = 4) or δ subunits (0.1 μg, to allow for comparable levels of protein expression; Fig. 4, *bottom row*; *n* = 6), FRET between β2^{HA} subunits was

completely eliminated, whereas FRET between individual $\alpha1^{HA}$ subunits persisted but was reduced. FRET was not detected between individual $\gamma2L^{HA}$ or δ^{HA} subunits (Fig. 4, *right column*), suggesting that either a single $\gamma2L^{HA}$ or δ^{HA} subunit was incorporated per pentamer or, alternatively, that two $\gamma2L^{HA}$ or δ^{HA} subunits were incorporated but separated by either an $\alpha1$ or $\beta2$ subunit.

To determine whether non-identical subunits could generate a FRET signal in $\alpha1\beta2$, $\alpha1\beta2\gamma2L$, and $\alpha1\beta2\delta$ receptors, a similar but separate set of experiments was performed. These experiments involved co-staining these same transfection combinations, except with donor-conjugated HA antibody and acceptor-conjugated $\alpha1$ or $\beta2$ subunit antibodies. For example, when the $\alpha1^{HA}\beta2$ condition was co-stained with donor-conjugated anti-HA and acceptor-conjugated anti-$\beta2$, a robust FRET signal was identified ($n = 4$). Taking a similar approach with $\alpha1\beta2\gamma2L$ ($n = 4$) and $\alpha1\beta2\delta$ ($n = 6$) receptors, all possible combinations of non-identical subunit FRET were identified, including between $\alpha1^{HA} \rightarrow \beta2$, $\beta2^{HA} \rightarrow \alpha1$, $\gamma2L^{HA} \rightarrow \alpha1$, $\gamma2L^{HA} \rightarrow \beta2$, $\delta^{HA} \rightarrow \alpha1$, and $\delta^{HA} \rightarrow \beta2$ subunits (donor $\rightarrow$ acceptor; data not shown). In summary, the FRET profiles of $\alpha1\beta2\gamma2L$ and $\alpha1\beta2\delta$ receptors were strikingly similar for all identical and non-identical subunit combinations, suggesting similar underlying subunit stoichiometries and arrangements.

10-Fold Difference in $\gamma2L^{HA}$ and δ^{HA} Subunit Expression Levels Did Not Reflect Differences in the Efficiency of Subunit Incorporation into Ternary Receptors—There are two possible explanations for the lower amounts of δ subunit cDNA required to recapitulate the flow cytometry expression patterns seen with the $\gamma2L$ subunit (Figs. 3 and 4). Either δ subunits are incorporated more efficiently into ternary GABA$_A$ receptors than $\gamma2L$ subunits or higher δ subunit levels are available for incorporation per unit of cDNA transfected, possibly because of increased subunit transcription, increased subunit translation, or decreased subunit degradation.

To test the first of these hypotheses, HEK293T cells were transfected with varying concentrations of $\gamma2L^{HA}$ or δ^{HA} subunit cDNA in the absence of $\alpha1$ or $\beta2$ subunits, and total cellular expression levels were evaluated using flow cytometry. Indeed, if the previous findings were related to more efficient incorporation of δ subunits into ternary receptors, then the discrepancy between $\gamma2L$ and δ subunit levels should not be observed when the subunits are expressed alone. However, we found that total cellular expression of δ^{HA} subunits (*solid gray line*) was significantly higher than that of $\gamma2L^{HA}$ subunits (*solid black line*) at all points when less than 1 μg of subunit cDNA was transfected (Fig. 5B, *circles*; $n = 4$). For instance, fluorescence levels detected when 0.03 μg of δ^{HA} cDNA was transfected were nearly identical to those detected when 0.3 μg of $\gamma2L^{HA}$ cDNA was transfected. Thus, the 10-fold difference in $\gamma2L^{HA}$ and δ^{HA} subunit expression levels (Fig. 3) persisted in the absence of partnering subunits, suggesting that differences in the efficiency of subunit incorporation did not account for the previous findings.

10-Fold Difference in GABA$_A$ Receptor $\gamma2L^{HA}$ and δ^{HA} Subunit Total Cellular Expression Could Not Be Accounted for by Differences in cDNA Transcription or Translation—To determine whether the difference between $\gamma2L^{HA}$ and δ^{HA} expres-
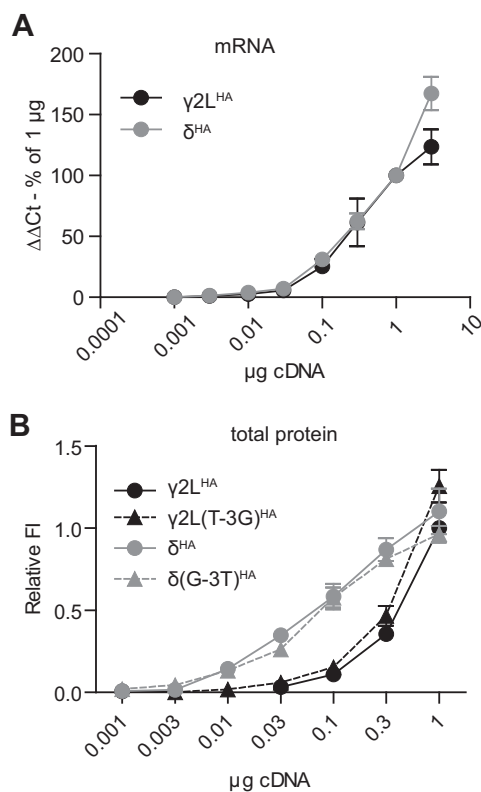
FIGURE 5. **10-Fold difference in total cellular expression of $\gamma2L^{HA}$ and δ^{HA} subunit protein persisted in the absence of partnering subunits and was not due to different rates of transcription or translation.** *A,* RNA was extracted from HEK293T cells transfected with 0.001–3 μg of $\gamma2L^{HA}$ (*black line*) or δ^{HA} (*gray line*) cDNA, and relative mRNA levels of each subunit were determined by real time PCR. The *x* axis indicates the amount of subunit cDNA transfected, and the *y* axis indicates the $\Delta\Delta Ct$ for subunit RNA normalized to the value for 1 μg of cDNA. All mRNA levels were normalized to housekeeping genes. *B,* flow cytometry was used to detect total cellular levels of $\gamma2L^{HA}$ (*solid black line*) and δ^{HA} (*solid gray line*) subunits when 0.001–3 μg of subunit cDNA was transfected in the absence of partnering $\alpha1$ and $\beta2$ subunits. To determine whether translation initiation due to Kozak sequences could affect subunit expression levels, the experiments were repeated after the Kozak sequences were swapped ($\gamma2L(T-3G)^{HA}$, *dashed black line*; $\delta(G-3T)^{HA}$, *dashed gray line*). All mock-subtracted fluorescence intensities were normalized to that of cells transfected with 1 μg of $\gamma2L^{HA}$ subunit cDNA.

sion levels was a result of more efficient transcription, real time PCR was performed on cells transfected over the same range of subunit cDNA used in the single subunit studies. Transcript levels were determined by normalized difference in cycle number fold increase. As cDNA levels increased, mRNA levels for $\gamma2L^{HA}$ and δ^{HA} subunits increased similarly and proportionally (Fig. 5A; $n = 4$), indicating that equivalent amounts of $\gamma2L^{HA}$ and δ^{HA} cDNA did not produce different amounts of protein because of differences in transcription efficiency.

To determine whether the difference between $\gamma2L^{HA}$ and δ^{HA} expression levels was a result of more efficient translation, we began by closely comparing the sequences of the cDNA constructs employed. Indeed, levels of protein expression in heterologous systems are known to be exquisitely sensitive to the design of the nucleic acid construct. For instance, if the $\gamma2L^{HA}$ coding sequence and untranslated regions were significantly longer than those of the δ^{HA} subunit, then equimolar amounts of plasmid DNA might not represent equimolar amounts of subunit cDNA. Full sequencing confirmed that the $\gamma2L^{HA}$ and δ^{HA} subunit inserts (translated and untranslated

sequences) were approximately the same length. However, the sequences of the immediate 5′-untranslated regions differed slightly between γ2L^{HA} and δ^{HA} subunit cDNAs. This could be problematic, because the 3 bp preceding and 2 bp following a start codon constitute the Kozak sequence, which contributes to the efficiency of translation initiation. Specifically, ribosome binding is strongly enhanced by the presence of purines at the −3 and +4 positions with respect to the start codon (40). In our cDNA constructs, the Kozak sequence of the γ2L^{HA} subunit cDNA was TCC(AUG)A, whereas the corresponding sequence of the δ^{HA} subunit cDNA was GCC(AUG)G; consequently, the δ^{HA} subunit would be predicted to be translated more efficiently than the γ2L^{HA} subunit.

To determine whether the Kozak sequence differences could account for the findings, the Kozak sequences of the γ2L and δ subunits were swapped. Therefore, the plasmids were engineered such that the γ2L^{HA} construct contained the Kozak sequence GCC(AUG)G and the δ^{HA} construct contained the Kozak sequence TCC(AUG)G (γ2L(T-3G)^{HA} and δ(G-3T)^{HA}, respectively. The single subunit titration experiments were then repeated using the γ2L(T-3G)^{HA} and δ(G-3T)^{HA} constructs. Surprisingly, the Kozak sequence mutations had little effect on total subunit expression levels. There was no significant difference between γ2L^{HA} (Fig. 5B, *solid black line, circles*) and γ2L(T-3G)^{HA} (Fig. 5B, *dotted black line, triangles*; n = 4) or between δ^{HA} (Fig. 5B, *solid gray line, circles*; n = 4) and δ(G-3T)^{HA} (*dotted gray line, triangles*; n = 4) subunit levels at any tested amount of subunit cDNA. Therefore, the 10-fold difference in GABA$_A$ receptor γ2L^{HA} and δ^{HA} subunit expression could not be attributed to differences in subunit synthesis at the stage of transcription or translation initiation.

However, it is possible that the subsequent *rate* of protein synthesis differed significantly and thus was responsible for the higher levels of δ subunit protein. To explore this possibility, HEK293T cells transfected with 1 μg of either γ2L^{HA} or δ^{HA} subunit cDNA were incubated for 0–20 min in media containing 150 μCi/ml [^{35}S]methionine (Fig. 6A; n = 4). At 5-min intervals, radiolabeled GABA$_A$ receptor subunit protein was precipitated by incubation with anti-HA beads. After elution, protein was subjected to SDS-PAGE and exposed to a phosphor screen. Integrated band density for each time point was calculated and normalized to the integrated band density of γ2L^{HA} subunits that were radiolabeled for 20 min (Fig. 6B; n = 4). When subunit expression levels at each time point were directly compared, δ^{HA} subunit levels were greater than γ2L^{HA} subunit levels at the 5-, 10-, and 15-min time points (p < 0.01) but not at the 20-min time point. This difference was surprising given that both subunits were engineered with identical plasmids and therefore regulated by identical promoters. Although difficult to explain, it should be noted that observed differences between γ2L^{HA} and δ^{HA} subunit levels in these experiments were relatively small and were insufficient to account for the 10-fold difference in expression levels seen in prior experiments. Moreover, when the synthesis curves were fitted using a mixed procedure model produced in consultation with the Vanderbilt University Department of Biostatistics, the synthesis curve slopes (which are most indicative of the rate of subunit synthesis) were not significantly different (p = 0.099).
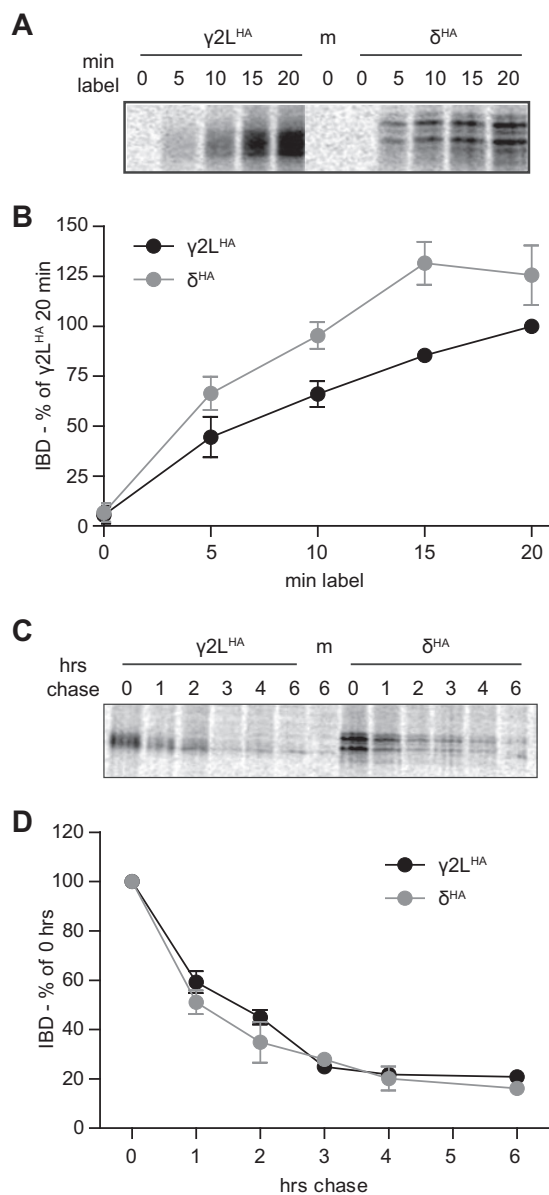
FIGURE 6. **GABA$_A$ receptor γ2L^{HA} and δ^{HA} subunits were synthesized at similar rates, and when newly synthesized, were degraded at similar rates.** Metabolic labeling was used to assess the synthesis and degradation rates of γ2L^{HA} and δ^{HA} subunits. *A* and *B*, HEK293T cells expressing equivalent amounts of γ2L^{HA} and δ^{HA} subunits were cultured for 0–20 min in media containing [^{35}S]methionine. Subunit protein was isolated from cell lysates by immunoprecipitation and separated by SDS-PAGE. *A* presents a representative gel exposure; *B* presents a quantification of band intensity (*IDV*) averaged from four separate experiments. Band intensities were normalized to those of the 20-min incubation condition. *C*, HEK293T cells expressing equivalent amounts of γ2L^{HA} or δ^{HA} subunits were cultured for 20 min in media containing [^{35}S]methionine. To assess degradation rates of this newly synthesized protein population, radioactive media were subsequently replaced by regular media, and cells were returned to incubators for 0–6 h. Subunit protein was isolated from cell lysates by immunoprecipitation and separated by SDS-PAGE. *C* presents a representative gel exposure, and *D* presents a quantification of band intensity (*IDV*) averaged from four separate experiments. Band intensities are normalized to that of the 0-min chase condition.

10-Fold Difference in GABA$_A$ Receptor γ2L^{HA} and δ^{HA} Subunit Total Cellular Expression Was Primarily Secondary to Differences in the Rate of Steady-state Subunit Degradation—Because the prior experiments detected no significant difference in the rates of γ2L^{HA} and δ^{HA} subunit transcription or transla-
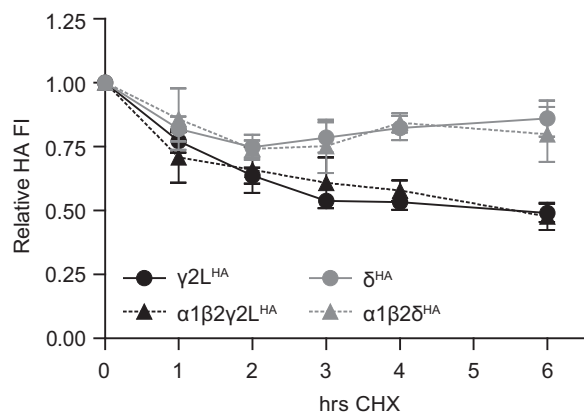
FIGURE 7. **GABA$_A$ receptor $\gamma2L^{HA}$ and δ^{HA} subunit steady-state pools had markedly different rates of degradation.** To assess degradation rates of the entire steady-state pool of GABA$_A$ receptor subunits, HEK293T cells allowed to express $\gamma2L^{HA}$ or δ^{HA} subunits for 48 h were then incubated for 0–6 h in the presence of 300 μM CHX. After incubation, cells were harvested, stained with anti-HA-Alexa-647 antibody, and analyzed by flow cytometry. Mock-subtracted mean fluorescence intensities from each time point were normalized to that of the same subunit at the 0-h time point.

tion, we next explored whether differences in subunit degradation could account for the findings using a pulse-chase assay. HEK293T cells transfected with 1 μg of either $\gamma2L^{HA}$ or δ^{HA} subunit cDNA were incubated for 20 min in radioactive media. Subsequently, the radioactive medium was replaced with normal culture medium, and cells were returned to the incubator. After 0 and 1–4 or 6 h, $\gamma2L^{HA}$ and δ^{HA} subunit proteins were extracted, immunoprecipitated, and processed as described above (Fig. 6C; $n = 4$). Integrated band density for each subunit was calculated and normalized to the 0-h time point. Both subunits had a half-life of ~1.5 h and decayed with essentially identical time courses (Fig. 6D; $n = 4$). It should be noted that a similar decay course has been reported for γ2S subunits (41). Thus, it initially seemed that subunit degradation could not account for the differing levels of $\gamma2L^{HA}$ and δ^{HA} subunit expression.

However, the pulse-chase technique only measures the degradation rate of proteins synthesized during the labeling period (*i.e.* subunits that may not have had sufficient time to be completely processed and trafficked). To evaluate degradation rate of the entire cellular pool of $\gamma2L^{HA}$ and δ^{HA} subunits, a variation of the previously described flow cytometry assay was employed. HEK293T cells were transfected with $\gamma2L^{HA}$ and δ^{HA} subunit cDNA and cultured as in previous experiments. Two days after transfection, 100 μg/ml cycloheximide (CHX)[3] was added to the culture medium to inhibit protein synthesis for 0–6 h before being harvested. Cells were then permeabilized, incubated with antibodies, and analyzed using flow cytometry. In contrast to the results obtained using the pulse-chase protocol, the flow cytometry CHX assay demonstrated that $\gamma2L^{HA}$ subunits degraded more rapidly than δ^{HA} subunits (Fig. 7; $n = 4$). During the 1st h of treatment, both subunits declined similarly. After 1 h, $\gamma2L^{HA}$ subunit levels (Fig. 7, *solid black line, circles*) had decreased to 77.2 ± 4.4% of 0-h levels, whereas δ^{HA} subunit levels (*solid gray line, circles*) had

decreased to 81.9 ± 4.8% of 0-h levels. After this point, degradation time courses diverged. After 6 h, δ^{HA} subunit levels remained stable at ~80% of 0-h levels (6 h of CHX, 86.0 ± 7.1%). In contrast, after 3 h of CHX treatment, $\gamma2L^{HA}$ subunit levels were approximately half (53.8 ± 2.3%) of 0-h levels, and they remained similar through the rest of the 6-h treatment period (6 h, 49.1 ± 3.5% of 0-h levels).

One possible explanation for these findings relates to the different cellular distributions of $\gamma2L^{HA}$ and δ^{HA} subunits when transfected alone (Fig. 1). Specifically, in the absence of α1 and β2 subunits, $\gamma2L^{HA}$ subunits were mostly retained intracellularly, but many δ^{HA} subunits were trafficked to the cell surface. Given that a substantial fraction of the intracellular subunit pool is likely destined for proteasomal degradation, the different degradation rates of $\gamma2L^{HA}$ and δ^{HA} subunits might simply reflect their different cellular distributions. If so, $\gamma2L^{HA}$ and δ^{HA} subunits would be expected to degrade at similar rates when expressed together with α1 and β2 subunits, which enabled maximal surface expression of all subunits. However, repeating the experiment in the setting of α1 and β2 subunit co-expression did not affect degradation rates of either $\gamma2L^{HA}$ or δ^{HA} subunits (Fig. 7; $n = 4$). The $\gamma2L^{HA}$ subunit population (Fig. 7, *dashed black line, triangles*) decreased by nearly half after 3 h of CHX application ($\gamma2L^{HA}$ = 53.8 ± 2.3% of 0 h; $\alpha1\beta2\gamma2L^{HA}$ = 60.8 ± 9.9% of 0 h) and then remained similar until the 6-h time point ($\gamma2L^{HA}$ = 49.1 ± 3.5% of 0 h; $\alpha1\beta2\gamma2L^{HA}$ = 47.7 ± 5.3% of 0 h). Likewise, δ^{HA} levels (Fig. 7, *dashed gray line, triangles*) decreased by around 20% within the 1st h of treatment (1 h, δ^{HA} = 81.9 ± 4.8% of 0 h; $\alpha1\beta2\delta^{HA}$ = 85.8 ± 12.0% of 0 h) and then remained stable until the 6-h time point (δ^{HA} = 86.0 ± 7.1% of 0 h; $\alpha1\beta2\delta^{HA}$ = 79.8 ± 10.7% of 0 h). Thus, the different degradation rates of $\gamma2L^{HA}$ and δ^{HA} subunits are likely intrinsic to the proteins themselves rather than a consequence of their differing subcellular distributions.

Very Low Levels of the δ Subunit Were Required to Eliminate the Functional Signature of $\alpha1\beta2$ Receptors—The findings in the previous sections indicated that very low levels of δ subunit cDNA were necessary to achieve high levels of expression, reflecting slower degradation as compared with the γ2L subunit. This suggested that low levels of the δ subunit would be required to eliminate the functional signature of $\alpha1\beta2$ receptors. To test this hypothesis, HEK293T cells were co-transfected with fixed levels of α1 and β2 subunit cDNA (1 μg per subunit) and variable concentrations (0.01–1 μg) of δ subunit cDNA. All cDNA constructs included non-HA-tagged sequences to allow comparison with previously reported results, as well as subsequent studies using the available concatenated cDNA constructs. GABA was applied for 4 s (Fig. 8A), and whole cell currents were analyzed for peak current amplitude (Fig. 8B) as well as macroscopic kinetic properties, including rise time (Fig. 8C), extent of desensitization (Fig. 8D), and deactivation time course (Fig. 8E). It should be noted that although experiments were conducted with the electrophysiologist blinded to transfection conditions, this proved impossible for cells transfected with the highest tested levels of δ subunit cDNA (1 μg) due to widespread cell death and abnormal morphology. Furthermore, the effects of >1 μg of δ subunit

---

[3] The abbreviations used are: CHX, cycloheximide; DZP, diazepam; BisTris, 2-[bis(2-hydroxyethyl)amino]-2-(hydroxymethyl)propane-1,3-diol.
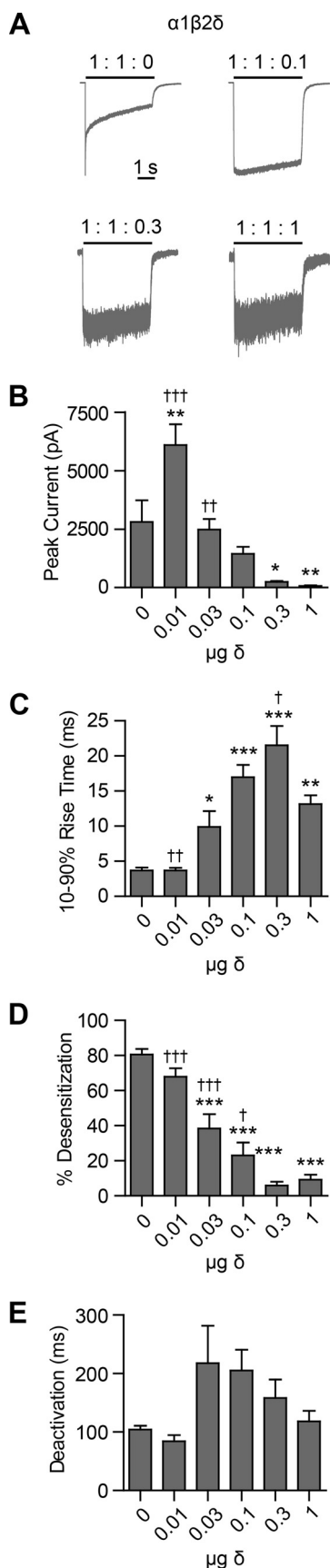
FIGURE 8. **Low levels of δ subunit cDNA were sufficient to eliminate kinetic signatures of α1β2 receptors.** GABA (1 mM; 4 s) was applied to HEK293T cells transfected with 1 μg of α1, 1 μg of β2, and varying amounts of δ subunit cDNA (*A*). Whole cell currents were recorded and analyzed to determine peak current amplitude (*B*); 10–90% rise time (*C*); percent fast desensitization (*D*) over 4 s from peak amplitude; and weighted time constant of deactivation (*E*). Representative currents from a subset of transfection conditions are presented in *A*. *, $p < 0.05$; **, $p < 0.01$; ***, $p < 0.001$ *versus* 1:1:0 and †, $p < 0.05$; ††, $p < 0.01$; †††, $p < 0.001$ *versus* 1:1:1.

cDNA could not be tested due to nearly universal death and poor membrane integrity of surviving cells.

Although flow cytometry using cells transfected with δ subunit cDNA showed surface δ subunit expression, these cells had no detectable GABA-evoked currents ($n = 5$). Similarly, no GABA-evoked current was obtained from cells co-transfected with α1 and δ subunit cDNAs ($n = 6$) or from cells co-transfected with β2 and δ subunit cDNAs ($n = 4$) (data not shown). Along with the flow cytometry results reported above, these data suggest a negligible contribution of any endogenous β subunit expression to our results. Very low levels of δ subunit cDNA produced significant changes in macroscopic current properties when co-transfected with α1 and β2 subunit cDNAs (Fig. 8). Cells expressing only α1 and β2 subunits produced currents with peak amplitudes of 2811 ± 921 pA ($n = 7$). However, when just 0.01 μg of δ subunit cDNA was included, peak current amplitudes increased significantly to 6099 ± 880 pA ($n = 6$, $p < 0.01$ compared with 1:1:0 μg condition). When 0.03 μg of δ subunit cDNA was included, peak current amplitude was 2477 ± 453 pA ($n = 8$), similar to the 1:1:0 μg condition. When still more δ subunit cDNA was included, peak current amplitudes continued to decline, with equimolar transfection yielding peak current amplitudes of only 68.8 ± 24.1 pA ($n = 6$, $p < 0.01$ compared with 1:1:0 μg condition). Although this precipitous drop in current amplitude mirrors the loss of receptor surface expression seen in the flow cytometry experiments, the possibility that altered receptor kinetic properties were contributing to loss of current amplitude cannot entirely be excluded.

As δ subunit cDNA levels increased, 10–90% rise times also changed, becoming progressively slower. When only α1 and β2 subunits were transfected, currents had an average rise time of 3.7 ± 0.4 ms ($n = 7$), but when 0.03 μg of δ subunit cDNA was included, average rise time slowed to 9.9 ± 2.2 ms ($n = 8$, $p < 0.05$ compared with the 1:1:0 transfection condition). In the 1:1:0.3 transfection condition, the average rise time further slowed to 21.5 ± 2.7 ms ($n = 5$, $p < 0.001$ compared with 1:1:0 transfection condition). Interestingly, the average rise time in the 1:1:1 transfection condition was faster than the 1:1:0.3 ($p < 0.01$) but slower than the 1:1:0 condition (13.1 ± 1.2 ms; $n = 6$), suggesting that the highest δ subunit cDNA transfection levels introduced a kinetically distinct αβδ receptor population.

It is commonly accepted that α1β$_x$ receptor currents desensitize far more extensively than α1β$_x$δ receptor currents (1). In agreement, increasing levels of δ subunit cDNA resulted in progressively decreasing extents of current desensitization. In the 1:1:0 μg transfection condition, currents desensitized by 80.5 ± 3.2% ($n = 7$), and in the 1:1:1 μg transfection condition, currents desensitized by only 9.2 ± 3.0% ($n = 6$). In all conditions other than 1:1:0.01 μg, desensitization was significantly different from that of the 1:1:0 μg condition ($p < 0.001$).

Finally, the time course of current deactivation was fitted for all transfection conditions and weighted deactivation time constants were calculated. In previous studies, α1β3 and α1β3δ receptors deactivated at similar rates (1), so it was perhaps unsurprising that there were no significant differences in deactivation time constants among all transfection conditions. However, there was a trend toward slower deactivation with increasing δ subunit cDNA, which was maximal when the 1:1:0.03 ratio of δ subunit cDNA was transfected (217.5 ± 64.2 ms, $n = 8$, compared with 1:1:0, 104 ± 6.8 ms; $n = 6$), after which there was a change in the trend toward faster deactivation with the highest level of δ subunit cDNA.

Taken together, these findings suggested that co-transfection of only 0.03 μg of δ subunit cDNA was sufficient to essentially eliminate the functional signature of α1β2 receptors. Whether this represented a truly homogeneous α1β2δ receptor population, however, remained unclear, as macroscopic current kinetic properties continued to change beyond this point, raising the possibility that alternative αβδ receptor isoforms could be formed in the presence of high δ subunit cDNA levels. Indeed, transfection with the highest amounts of δ subunit cDNA resulted in alterations of macroscopic current kinetic properties. Unfortunately, the marked associated decrease in current amplitude with increasing levels of δ subunit cDNA significantly limited detailed kinetic analysis, particularly at the highest transfection levels.

Low Levels of the γ2 Subunit Were Required to Eliminate the Functional Signature of α1β2 Receptors—To determine the cDNA transfection ratio at which the functional signature of α1β2 receptors was eliminated in the presence of the γ2 subunit, and to explore the possibility that the kinetic properties of γ2 subunit-containing receptors were also sensitive to transfection ratio, HEK293T cells were co-transfected with α1 and β2 subunits (1 μg per subunit) and variable amounts (0.01–10 μg) of the γ2S subunit. (Of note, using the γ2S instead of the γ2L subunit allowed us to directly compare the electrophysiology results to those obtained from the available tandem constructs used in subsequent experiments. No significant difference was found in the kinetic properties of these splice variants; data not shown.) GABA was applied for 4 s (Fig. 9A), and whole cell currents were analyzed for peak current amplitude (Fig. 9B) as well as macroscopic kinetic properties including rise time (Fig. 9C), extent of desensitization (Fig. 9D), and deactivation time course (Fig. 9E). As with the δ subunit experiments, the electrophysiologist was blinded to transfection conditions, but again, this proved impossible for cells transfected with the highest tested levels of γ2S subunit cDNA (10 μg) due to widespread cell death.

As with the δ subunit electrophysiology experiments, peak current amplitudes were significantly affected by even low amounts of γ2S subunit cDNA transfected. For example, although cells transfected with only α1 and β2 subunit cDNAs had peak current amplitudes of 814 ± 266 pA ($n = 14$) (Fig. 9, A and B), addition of just 0.01 μg of γ2 subunit cDNA significantly increased peak current amplitude to 3510 ± 682 pA ($n = 17$, $p < 0.05$). Although this marked increase in current amplitude with very low levels of the γ2 subunit appeared surprising given the minimal associated change in receptor surface levels,

this likely reflects the much higher charge transfer mediated by α1βγ2 receptors (~7-fold higher than α1β2 receptors) secondary to increased single channel conductance and gating differences (29). For example, if just 15% of surface α1β2 receptors are converted into α1β2γ2L receptors, current amplitude would be expected to nearly double. Higher γ2 subunit cDNA levels yielded similar increases in current amplitudes (all γ2 subunit cDNA amounts from 0.01 to 3 μg produced currents that were significantly larger than α1β2 currents), with the largest peak current observed in the 1:1:0.3 μg transfection condition (5866 ± 761 pA; $n = 14$, $p < 0.001$ compared with α1β2). Interestingly, there was a strong trend toward decreasing amplitude with high γ2 subunit cDNA amounts above 0.3 μg. For the 1:1:10 μg transfection condition, peak current amplitude was only 2870 ± 480 pA ($n = 21$), which was ~50% lower than the peak current amplitude seen in the 1:1:0.3 μg transfection condition (4530 ± 483 pA; $n = 25$). Although it seems likely that this decrease in current amplitude was at least partly accounted for by loss of receptors on the cell surface given the flow cytometry results, the degree to which current amplitude was reduced is less than that seen for surface expression, raising the possibility that intrinsic channel kinetic properties had changed at the highest transfection ratios.

Like peak current amplitudes, low amounts of γ2 subunit cDNA were sufficient to alter current rise times. The average 10–90% rise time (Fig. 9C) of α1β2 receptor currents was 2.47 ± 0.19 ms ($n = 14$). Although this remained similar for the 1:1:0.01 μg transfection condition (2.23 ± 0.15 ms; $n = 13$), the rise time decreased for the 1:1:0.03 μg transfection condition (1.00 ± 0.10 ms; $n = 9$, $p < 0.01$). Rise times were similar (~1 ms) when 0.03–1 μg of γ2 subunit cDNA was transfected, but it began trending upward when γ2 subunit cDNA was transfected in excess. At 1:1:3 μg, the 10–90% rise time was 1.79 ± 0.31 ms ($n = 5$), slightly slower than that of the 1:1:1 μg transfection condition (1.48 ± 0.13 ms; $n = 15$), although this difference did not reach significance. However, the 1:1:10 μg transfection condition yielded the slowest rise times of any condition (3.48 ± 0.47 ms; $n = 18$; $p < 0.05$ compared with 1:1:0 and $p < 0.001$ compared with 1:1:1). Thus, although rise times decreased initially with increasing γ2 subunit levels, they eventually increased when γ2 subunits were expressed in excess, again suggesting that α1β2γ2 receptors with distinct kinetic properties were formed at the highest expression levels.

According to most reports, αβ and αβγ receptors both desensitize extensively; however, αβ receptors desensitize more rapidly. To determine whether a shift from α1β2 to α1β2γ2 receptor populations could be detected by changes in desensitization kinetics, 1 mM GABA was applied for 4 s to transfected cells, and the desensitization time course of resulting currents was fitted with up to four exponential components. The percent of all desensitization contributed by the two shorter components (τ1 and τ2, ≤16 and 17–125 ms, respectively) was summed and defined as fast desensitization (Fig. 9D). For α1β2 receptors, 65% of all desensitization was contributed by the two shorter components, and this fraction dropped significantly when 0.01 μg of γ2 subunit cDNA was co-expressed (50 ± 5%, $p < 0.05$). Only 0.03 μg of γ2 subunit cDNA was necessary to reduce fast desensitization to levels statisti-
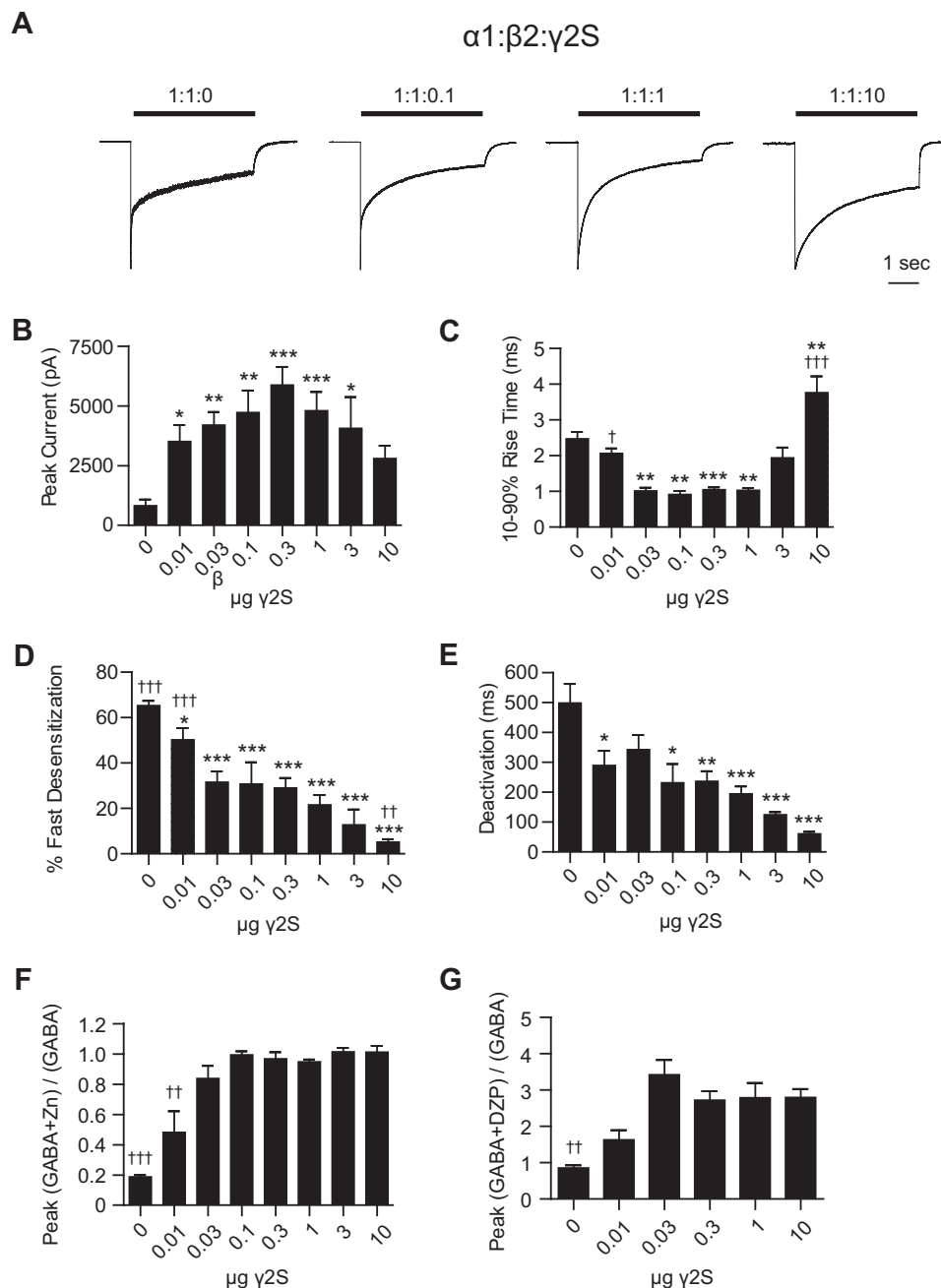
Biogenesis of Synaptic αβγ and Extrasynaptic αβδ Receptors

FIGURE 9. **Low levels of γ2 subunit cDNA were sufficient to eliminate kinetic and pharmacological signatures of $\alpha1\beta2$ receptors.** GABA (1 mM; 4 s) was applied to HEK293T cells transfected with 1 μg of $\alpha1$, 1 μg of $\beta2$, and varying amounts of γ2S subunit cDNA (*A*). Whole cell currents were recorded and analyzed to determine peak current amplitude (*B*); 10–90% rise time (*C*); percent fast desensitization (*D*) over 4 s from peak amplitude; and weighted time constant of deactivation (*E*). Representative currents from a subset of transfection conditions are presented in *A*. *F,* HEK293T cells transfected with 1 μg of $\alpha1$, 1 μg of $\beta2$, and varying amounts of γ2S subunit cDNA were pretreated (10 s) with Zn^{2+} (10 μM), and currents were recorded during a 4-s co-application of GABA (1 mM) and Zn^{2+} (10 μM). Zn^{2+} resistance was calculated by dividing the peak current amplitude in response to GABA + Zn^{2+} by the peak current amplitude in response to GABA alone. *G,* currents were recorded from HEK293T cells transfected with 1 μg of $\alpha1$, 1 μg of $\beta2$, and varying amounts of γ2S subunit cDNA during a 4-s co-application of GABA ($\sim EC_{20}$) and DZP (1 μM). DZP enhancement was expressed as the ratio of peak current amplitude in response to GABA + DZP divided by the peak current amplitude in response to GABA alone. *, $p < 0.05$; **, $p < 0.01$; ***, $p < 0.001$ *versus* 1:1:0 and †, $p < 0.05$; ††, $p < 0.01$; †††, $p < 0.001$ *versus* 1:1:1.

cally indistinguishable from those produced by 1 μg of γ2 subunit cDNA (32 ± 5 and 23 ± 5%, respectively). Interestingly, 10 μg of γ2 subunit cDNA further reduced fast desensitization, to a level that was significantly lower than 1 μg (5 ± 1%, $p < 0.01$). Thus, similar to the results for current rise time, analysis of fast desensitization demonstrated that low levels of γ2 subunit cDNA were sufficient to eliminate the functional signature of

$\alpha1\beta2$ receptors and that increasing levels of γ2 subunit cDNA continued to change kinetic properties again, implying the presence of one or more alternative receptor isoforms when γ2 subunit cDNA was transfected in excess.

The weighted time constant of deactivation also changed dramatically in response to the amount of γ2 subunit cDNA that was transfected (Fig. 9*E*). Specifically, when more γ2 sub-

unit cDNA was transfected, currents deactivated more rapidly (*i.e.* the weighted deactivation time constant decreased). For instance, the 1:1:0 μg transfection condition produced $\alpha 1\beta 2$ receptor currents with a deactivation time constant of 498 ± 64 ms, whereas the 1:1:1 μg transfection condition produced currents with a deactivation time constant of 163 ± 27 ms and the 1:1:10 μg transfection condition produced currents with a deactivation time constant of 68 ± 8 ms. Thus, much like the patterns seen with desensitization, deactivation progressively changed throughout the tested range of $\gamma 2$ subunit cDNA levels.

Low γ2 Subunit cDNA Levels Eliminated the Pharmacological Signature of α1β2 Receptor Isoforms—There are two established methods for distinguishing $\alpha\beta$ and $\alpha\beta\gamma$ receptor isoforms pharmacologically. First, $\alpha\beta$ receptor currents are strongly inhibited by Zn^{2+} (42), whereas $\alpha\beta\gamma$ receptor currents are not. In contrast, $\alpha\beta$ receptors are insensitive to diazepam (DZP), reflecting the absence of an α-γ subunit interface, whereas diazepam significantly enhances $\alpha 1,2,3,5\beta\gamma$ receptor GABA-evoked currents (43, 44). (Of note, $\alpha\beta\delta$ receptors are only partially Zn^{2+}-sensitive and DZP-insensitive, so these techniques could not be used to differentiate $\alpha\beta$ and $\alpha\beta\delta$ receptors.) To determine how much $\gamma 2$ subunit cDNA was necessary to eliminate the pharmacological signature of $\alpha\beta$ receptors, peak current amplitude in response to GABA (1 mM, 4 s) was recorded (I_{max}(GABA)); Zn^{2+} (10 μM) was pre-applied for 10 s, and peak current amplitude was recorded again although GABA and Zn^{2+} were co-applied (I_{max}(GABA + Zn^{2+})). Zn^{2+} inhibition was quantified by dividing I_{max}(GABA + Zn^{2+}) by I_{max}(GABA) (Fig. 9F). As expected, cells transfected with only $\alpha 1$ and $\beta 2$ subunits produced currents that were inhibited strongly by Zn^{2+} co-application (peak current amplitude was $19 \pm 1\%$ of those evoked by GABA alone). When 0.01 or 0.03 μg of $\gamma 2$ subunit cDNA was included, peak current amplitude was partially Zn^{2+}-sensitive (32 ± 13 and $84 \pm 9\%$ of I_{max}(GABA), respectively; $p < 0.001$ compared with $\alpha\beta$). When ≥ 0.1 μg of $\gamma 2$ subunit cDNA was included, peak current amplitude was maximally Zn^{2+}-insensitive, again suggesting that low $\gamma 2$ subunit levels were sufficient to eliminate the $\alpha\beta$ receptor population.

As mentioned previously, $\alpha\beta\gamma$ receptors are inhibited by Zn^{2+} but enhanced by DZP. We first characterized the GABA concentration-response relationships for a subset of stoichiometries. The GABA EC_{50} value of cells expressing only $\alpha 1$ and $\beta 2$ subunits was 8.1 μM (95% confidence interval = 6.1–10.7 μM; $n = 6$). Cells transfected with 1:1:1 $\alpha 1$:$\beta 2$:$\gamma 2$ had an EC_{50} of 13.9 μM (10.9–17.6 μM; $n = 7$). Cells transfected with 1:1:10 $\alpha 1$:$\beta 2$:$\gamma 2$ had an EC_{50} of 61.9 (41.2–92.2 μM; $n = 5$). To determine how much $\gamma 2$ subunit cDNA was necessary to produce a DZP-sensitive receptor population, the percent enhancement of ~EC_{20} GABA-evoked peak current amplitude by 1 μM DZP was evaluated (Fig. 9G). Even 0.01 μg of $\gamma 2$ subunit cDNA permitted substantial DZP potentiation of peak current amplitude ($134 \pm 13\%$ of control current), and 0.03 μg was sufficient to produce potentiation ($204 \pm 18\%$) indistinguishable from 1 μg ($260 \pm 26\%$) or 10 μg ($257 \pm 56\%$).

These experiments indicated that low levels of $\gamma 2$ subunit cDNA were necessary to eliminate the pharmacological signa-

tures of $\alpha 1\beta 2$ receptors. However, it should be emphasized that the observed transition point to a predominantly $\alpha\beta\gamma$ receptor population may be exaggerated in these experiments due to the aforementioned higher charge transfer associated with $\alpha 1\beta 2\gamma 2$ receptors (see above for $\alpha 1\beta 2\gamma 2$ electrophysiology experiments). Nevertheless, the results clearly demonstrate that excess $\gamma 2$ subunit was not required to eliminate the pharmacological signature of $\alpha 1\beta 2$ receptors. Interestingly, DZP potentiation reached a plateau at a transfection ratio of ~1:1:0.3 μg, meaning that any alternative $\alpha\beta\gamma$ receptor populations introduced at higher transfection ratios (as suggested by the aforementioned changes in macroscopic current kinetics) must be similarly DZP-sensitive, implying that the α-γ subunit interface must be preserved in those isoforms.

Expression of Concatenated Subunit Constructs Demonstrated That Alternate α1β2γ2 GABA$_A$ Receptor Stoichiometries Were Functional—The flow cytometry and electrophysiology subunit titration studies suggested the presence of alternative receptor isoforms at high levels of $\gamma 2$ or δ subunit expression, with kinetic properties distinct from those seen with low levels of $\gamma 2$ or δ subunit expression. Importantly, these conclusions were based entirely on results from experiments where receptor subunits were permitted to assembly freely. However, to confirm our suspicion that alternative *functional* stoichiometries and subunit arrangements were possible, we turned to cDNA constructs encoding concatameric GABA$_A$ receptor subunits, acknowledging the known technical limitations of this approach. For example, although concatenated subunits have the distinct advantage of constraining the arrangement of GABA$_A$ receptor subunit proteins, concern has been raised that linking peptides could potentially be cleaved, releasing individual subunits and invalidating any stoichiometric constraints. There is also concern that concatamers could remain physically intact but only partially incorporate into a receptor (*i.e.* become looped out of the receptor), again resulting in lack of stoichiometric constraint.

To address the first of these concerns, tandem constructs were expressed in HEK293T cells and detected with immunoblotting (of note, the flow cytometry assay could not be used to detect concatenated subunits, as the linkers markedly decreased subunit antibody binding, which is targeted to the N terminus). Proteins were identified at ~50-, 100-, and 150-kDa bands when individual GABA$_A$ receptor subunits, double-subunit concatamers, or triple-subunit concatamers were individually expressed, respectively, indicating that linker cleavage had not occurred. Moreover, no abnormal lower molecular weight bands were consistently identified to suggest partial protein cleavage (data not shown). With that said, it should be noted that despite adjusting cDNA transfection levels to compensate for construct size (see "Experimental Procedures"), individual subunits were expressed at much lower levels when they were incorporated into concatamers than when they were expressed as individual subunits. Consequently, we did not directly compare amplitudes of currents recorded from cells expressing concatameric subunits to those expressing freely assembled subunits. Based on the presence or absence of currents, however, electrophysiological recording should expose which sub-

		Imax (pA)	Rise (ms)	% Fast Desens	DZP : τ_{deact} Prolongation	Possible subunit arrangements
1	βαβ alone	None				
2	βαβ + α	None				
3	βαβ + β	None				
4	βαβ + γ	None				
5	α-γ alone	None				
6	α-γ + β	4246 ± 690 (n = 9)	2.05 ± 0.15 (n = 9)	9 ± 1% (n = 7)	88 ± 4% (n=6)	β-α-γ-α-γ
7	"Canonical" α-γ + β-α-β	1012 ± 272 (n=8)	2.71 ± 0.25 (n=8)	14 ± 2% (n=7)	214 ± 33% (n=7)	β-α-γ-β-α
8	β-α-γ alone	None				
9	β-α-γ + α	1187 ± 209 (n = 13)	2.57 ± 0.17 (n = 13)	19 ± 3% (n = 11)	147 ± 16% (n = 9)	β-α-γ-α-α
10	β-α-γ + β	None				
11	β-α-γ + γ	None				
12	β-α-γ + α + γ	668 ± 102 (n = 8)	2.47 ± 0.21 (n = 7)	5 ± 3% (n = 5)	59 ± 19% (n=3)	β-α-γ-α-α β-α-γ-α-γ
13	β-α-γ + β + γ	239 ± 68 (n = 9)	7.49 ± 0.05 (n = 8)	7 ± 6% (n = 5)	99 ± 32% (n = 6)	β-α-γ-β-γ

FIGURE 10. **Concatameric cDNA constructs were used to determine which α1β2γ2 subunit combinations could form functional GABA$_A$ receptors.** The various combinations of concatameric and single subunit constructs tested are shown along with their respective current kinetic properties and diazepam sensitivity (peak (I_{max}), rise time (*Rise*), desensitization (% *Fast Desens*), and effect of DZP on deactivation (τ_{deact} prolongation)). Note that peak current amplitudes should be interpreted with caution, as they are likely heavily influenced by receptor surface expression, which is markedly reduced for concatameric constructs. Only possible subunit arrangements that included a properly oriented β-α interface (for GABA binding) and α-γ interface (for benzodiazepine binding) are illustrated. Potential arrangements containing β-β and/or γ-γ subunit interfaces were deemed unlikely based on the FRET results.

unit combinations can theoretically form functional receptors and which cannot.

Currents were recorded from HEK293T cells expressing various combinations of β2-α1-β2, β2-α1-γ2, and α1-γ2 concatamers together with α1, β2, and/or γ2 monomers (see under "Experimental Procedures" for details of tandem construction). The combinations chosen were designed to constrain receptor assembly such that some conditions should not produce pentameric receptors, some should only produce "canonical" GABA$_A$ receptor isoforms (β-α-γ-β-α), and some could produce only alternative isoforms (of particular interest were those containing multiple γ2 subunits). For each condition, the possible isoforms and kinetic properties of resulting whole cell currents were listed in Fig. 10. Of note, we focused on γ2 subunit-containing concatameric constructs for several reasons. First, they had already been generated, optimized, and validated by the Sigel laboratory in combination with β2 subunits by the time of data acquisition, allowing for direct comparison to our results from freely assembled subunits, whereas δ subunit concatameric constructs were novel and only available in combination with β3 subunits, which could have confounded results due known differences in trafficking and assembly characteristics. Second, although α1βxγ2 receptors are the most abundant combination found in brain, the α1β2δ subunit combination has a limited distribution. Most δ subunit-containing receptors are partnered with α4 or α6 subunits, but using a non-α1 subunit subtype would have confounded our ability to elucidate the rules for δ/γ2 subunit incorporation. Third, given that expression of concatenated subunits tends to be low, γ2 subunit-containing concatameric constructs were preferred over δ subunit concatameric constructs due to their higher charge transfer, which should offset the lower expression levels. Finally, it should be emphasized that the flow cytometry data demonstrated nearly identical expression patterns with γ2 and δ subunits when expressed at equivalent levels, suggesting that ternary α1β2γ2 and α1β2δ receptors have similar subunit stoichiometries and arrangements.

To address the technical concern that individual subunits within a concatamer may "loop out," allowing double subunit constructs to incorporate into receptors as single subunits (or triple subunit constructs to incorporate as double subunits), we first evaluated currents from cells transfected with one tandem construct alone (*e.g.* β-α-β, α-γ, and β-α-γ; Fig. 10, *rows 1, 5, and 8*, respectively). In all conditions, no GABA-evoked currents were recorded. We next evaluated a concatamer combination that should only produce the canonical β-α-γ-β-α iso-

form (α-γ + β-α-β; Fig. 10, *row 7*), and we confirmed that it yielded a robust current (1012 ± 272 pA; *n* = 8). These control experiments suggested that these concatameric constructs assembled as predicted within HEK293T cells and could therefore be used to explore the possibility of alternative subunit stoichiometries and arrangements.

We were particularly interested in concatamer combinations that would yield ternary receptors containing more than one γ subunit, as our titration experiments suggested increasing γ levels progressively altered current kinetics. Consistent with this hypothesis, large currents were recorded from cells transfected with multiple concatamer combinations. For instance, when the α-γ construct was expressed together with a β monomer, whole cell currents averaged 4246 ± 690 pA (*n* = 9; Fig. 10, *row 6*). This combination is predicted to yield the β-α-γ-α-γ isoform, which has not been previously demonstrated to be functional. Although this transfection combination could theoretically also produce β-α-γ-β-β receptors, these were felt to be highly unlikely as this subunit arrangement should have yielded a robust β → β FRET signal in our flow cytometry studies; instead, we only identified β → β FRET with α1 and β2 subunit co-transfection (inclusion of either γ2 or δ subunits completely eliminated β → β FRET). Currents were also recorded when the β-α-γ triple subunit construct was transfected together with other subunit combinations incapable of forming canonical receptor isoforms. Co-expression of β-α-γ concatamers with α subunit monomers, a combination predicted to form β-α-γ-α-α receptors, yielded whole cell currents averaging 1187 ± 209 pA (*n* = 9; Fig. 10, *row 9*). Co-expression of β-α-γ concatamers with both α subunit and γ subunit monomers (possible receptors include β-α-γ-α-α and β-α-γ-α-γ, with β-α-γ-γ-γ receptors felt extremely unlikely given the absence of γ → γ FRET) produced whole cell currents averaging 668 ± 102 pA (*n* = 8; Fig. 10, *row 12*). Finally, co-expression of β-α-γ concatamers with both β subunit and γ subunit monomers (possible isoform: β-α-γ-β-γ, with β-α-γ-β-β and β-α-γ-γ-γ receptors felt extremely unlikely given the absence of β → β or γ → γ FRET) produced small but reproducible currents that were significantly different from zero (*n* = 9; Fig. 10, *row 13*). The concatamer electrophysiology data thus strongly supported the hypothesis that co-transfecting γ/δ subunits with α and β subunits can produce a heterogeneous mixture of functional receptors, rather than a single canonical β-α-γ/δ-β-α receptor.

Discussion

Flow Cytometry Provided an Efficient Quantitative Method for Evaluating GABA_A Receptor Subunit Expression—Among ion channels, GABA_A receptors are remarkable for their complexity. The 19 subunit subtypes, many of which are co-expressed in individual neurons, can theoretically produce a myriad of heteropentameric receptor isoforms. Determining which GABA_A receptor subunit combinations can traffic to the cell surface, and what the stoichiometries and arrangements are of these receptors, has thus presented a fascinating yet frustrating problem for investigators. Here, we demonstrate the utility of a flow cytometry assay for a high-throughput quantitative evaluation of subunit expression resulting from numerous transfec-

tion combinations. Flow cytometry can also serve as a surrogate for some traditional biochemistry techniques, as illustrated in our experiments comparing subunit degradation rates.

Using these flow cytometry-based assays, we demonstrated that γ2L and δ subunits were incorporated into ternary GABA_A receptors similarly when expressed at equivalent protein levels as follows: both required co-expression with α1 and β2 subunits for maximal surface expression; both incorporated into ternary receptors preferentially at the expense of β2 subunits; both yielded identical subunit FRET profiles, suggesting similar underlying stoichiometries and arrangements; and both exerted potent dominant negative effects on co-transfected subunits when expressed at high levels. The most striking difference between γ2L and δ subunits was their stability, the latter having a slower rate of degradation, and consequently higher levels of surface and total cellular expression at any given amount of cDNA transfected. We propose that this could represent an important regulatory mechanism for extrasynaptic αβδ receptors, which mediate "tonic" inhibitory currents and might therefore benefit from increased stability. Interestingly, δ subunits were also capable of reaching the cell surface when transfected alone, a phenomenon previously only described for β1/3, γ2S, and ρ1–3 subunits (33, 45–48).

Flow Cytometry Evaluation of GABA_A Receptor Subunit Expression Provided Evidence for Heterogeneous αβγ and αβδ Receptor Populations—The observation that increasing levels of γ2L or δ (subsequently γ2/δ) subunit cDNA progressively decreased β2, but not α1, subunit surface levels suggested that the position of β2 subunits in the pentamer was preferentially being replaced by γ2/δ subunits. Because α1β2 receptor stoichiometry is generally thought to be 2α:3β with β-α-β-β-α subunit arrangement (5), the simplest explanation would be that γ2/δ subunit incorporation yielded canonical 2α:2β:1γ2/δ receptors with β-α-γ/δ-β-α arrangement. However, this model was inconsistent with our quantitative flow cytometry data. Replacement of a single β2 subunit would be expected to decrease surface levels by at most 33%, whereas we observed an ~50% decrease without significant accompanying change in α1 subunit surface levels. This was followed by decreases in both α1 and β2 subunit surface levels at higher levels of γ2/δ subunit expression, despite progressively increasing γ2/δ subunit surface levels.

Given that α1β2 receptors must contain two GABA-binding β-α subunit interfaces (overwhelmingly supported by the literature) (49), these findings suggest the presence of a mixed population of 2α:3β and 3α:2β receptors with β-α-β-α-α and β-α-β-β-α arrangements (Fig. 11, *left-most column*), respectively, noting that both isoforms have previously been suggested (14). However, similar to our results (Fig. 10, *2nd row*), Baumann *et al.* (5) found that the β-α-β-α-α arrangement does not conduct GABA-evoked currents. This model would not only explain the α1β2 FRET data, which suggested the presence of both β-β and α-α subunit interfaces (Fig. 4), but would also explain the observed decreased β2 subunit surface levels (loss of one β2 subunit from each isoform would result in a 40% decrease in surface levels, possibly more if the 3α:2β was more prevalent). Moreover, this model could explain why β → β subunit FRET was completely eliminated with γ2/δ subunit co-transfection,

ASBMB

FIGURE 11. Subunit stoichiometry and arrangement of α1β2γ2 GABA$_A$ receptors depends on the relative expression level of γ2 subunits. A summary of the flow cytometry and electrophysiology data supporting the existence of alternative α1β2γ2 receptor isoforms is shown. In the absence of the γ2 subunit ("*No γ*", α:β:γ cDNA transfection ratio 1:1:0), α1β2 receptors represent a mixed population of 2α:3β receptors with β-α-β-β-α arrangement and 3α:2β receptors with β-α-β-α-α arrangement, the latter likely not functional (depicted as × through the pore of this receptor). With low levels of γ2 subunit expression ("*Low γ*", α:β:γ cDNA transfection ratio 1:1:≤1), incorporation of the γ2 subunit into the pentamer preferentially occurs at the expense of β2 subunits, resulting in formation of 2α:2β:1γ receptors with β-α-γ-β-α arrangement and 3α:1β:1γ receptors with a β-α-γ-α-α arrangement. At higher levels of γ2 subunit expression ("*High γ*", α:β:γ cDNA transfection ratio 1:1:≥1), γ2 subunits continue to replace β2 subunits but can also begin to replace α1 subunits, resulting mainly in formation of 2α:1β:2γ receptors with β-α-γ-α-γ arrangement. Of note, the results suggest that 1α:2β:2γ receptors with β-α-γ/δ-β-γ arrangement may also form (data not shown), but these are thought to represent a relatively minor population.

whereas α → α subunit FRET persisted. Indeed, although there is loss of β-β interfaces when 2α:3β receptors with β-α-β-β-α arrangement are converted to canonical 2α:2β:1γ/δ receptors with β-α-γ/δ-β-α arrangement, loss of a β2 subunit from 3α:2β receptors with β-α-β-α-α arrangement could only yield 3α:1β:1γ/δ receptors with a β-α-γ/δ-α-α arrangement (or the mirror image), which maintain an α-α interface (Fig. 11, *middle column*).

The observation that α1 subunit surface levels also began decreasing with α:β:γ/δ cDNA transfection ratios above 1:1:0.3/0.03 despite increasing γ2/δ subunit surface levels suggested that a second γ2/δ subunit could be incorporated into receptors at the expense of an α1 subunit (Fig. 11, *right-most column*). Of note, rising γ2/δ subunit surface levels could not be explained by independent trafficking of γ2/δ subunits, as they were not efficiently expressed on the surface when transfected alone at these same cDNA levels (single subunit surface expression titration data not shown; note that Fig. 1 shows expression levels for 1 μg of γ/δ cDNA only). For the aforementioned 3α:1β:1γ/δ receptors with β-α-γ/δ-α-α arrangement, replacing an additional α subunit with a γ/δ subunit would yield 2α:1β:2γ/δ receptors, likely with β-α-γ/δ-α-γ/δ arrangement (replacement of other α subunits with a γ/δ subunit would introduce adjacent γ/δ subunits, which would have yielded γ → γ/δ → δ FRET). For canonical 2α:2β:1γ/δ receptors with β-α-γ/δ-β-α arrangement, replacing an additional α subunit with a γ/δ subunit would yield 1α:2β:2γ/δ receptors with β-α-γ/δ-β-

γ/δ arrangement (replacement of the other α subunit would have yielded γ → γ/δ → δ FRET). Of note, β2 subunit surface levels decreased along with α1 subunits despite increasing γ2/δ subunit levels, suggesting that a second γ2/δ subunit could also be incorporated at the expense of β2 subunits. This was unlikely to involve the 3α:1β:1γ/δ isoform, as this would have yielded α1γ/δ receptors, which are retained intracellularly (Fig. 1). However, the 2α:2β:1γ/δ receptor with β-α-γ/δ-β-α arrangement could have lost a second β2 subunit, thereby providing an alternative pathway for forming the 2α:1β:2γ/δ isoform with β-α-γ/δ-α-γ/δ arrangement (loss of the other β2 subunit position would have yielded γ → γ/δ → δ FRET).

Electrophysiology experiments utilizing concatameric subunit constructs confirmed that all four of the proposed α1β2γ2 receptor isoforms were theoretically functional (Fig. 10). Of the double-γ subunit possibilities, β-α-γ-α-γ and β-α-γ-β-γ, the former is most likely the dominant receptor (Fig. 11, *right-most column*), as equal proportions should have yielded less pronounced β2 subunit loss and more prominent α1 subunit loss from the cell surface at high transfection ratios (Fig. 3). Although we did not perform analogous concatamer studies for αβδ receptors, the overwhelming similarity between the patterns of γ2L and δ subunit expression and adjacency argues strongly for similar underlying subunit stoichiometries and arrangements. With that said, future studies with concatameric δ subunit constructs will be important to evaluate which of the αβδ subunit arrangements are possible and to evaluate their

kinetic and pharmacological properties. Although there has been some work with concatameric constructs confirming that double-δ subunit receptors are theoretically possible (11, 13), direct comparison with our results is limited, as the identity of partnering subunits differed in those studies (*e.g. α1 versus α4; β2 versus β3*). Of note, differences in partnering subunit identity may also explain why prior studies have reported conflicting αβδ stoichiometries with increasing transfection ratios, some supporting the canonical 2:2:1 ratio (8, 9) but others supporting ratios up to 1:1:3 (11).

This study provides important insights into how the relative expression levels of individual subunit genes help determine the subunit stoichiometry and arrangement of functional surface GABA$_A$ receptors. Although we found a limited cohort of alternative pentameric assemblies, there are undoubtedly further constraints imposed when actually expressed in neurons. An important future direction of this work will be determining which, if any, of the alternative αβγ and αβδ isoforms exist *in vivo*. Very early immunoprecipitation studies of γ subunits from rodent brain suggested the presence of receptors containing multiple γ2 subunits (16). However, the presence of multiple γ2 subunits is predicted in our model to result in loss of the GABA-binding site and gain of a benzodiazepine-binding site (Fig. 11, *right column*), in contrast to early work with receptors isolated from bovine brain, which demonstrated a 2:1 ratio of GABA to benzodiazepine-binding sites (50). The presence of double-δ subunit receptors *in vivo* has not yet been explored to our knowledge. If alternative isoforms do occur outside of heterologous expression systems, it will be interesting to determine their relative proportions, subcellular localization, and functional and pharmacological properties and to determine how these properties are affected by disease-causing mutations (*e.g.* under/overexpressing GABA receptor subunit mutations associated with epilepsy). It will also be of interest to explore the mechanistic bases for the altered subunit stoichiometries and arrangements from the standpoint of receptor assembly.

Low Levels of γ2L and δ Subunit cDNA Were Sufficient to Eliminate the Functional Signature of α1β2 Receptors—There is ongoing debate in the GABA$_A$ receptor literature regarding the optimal subunit transfection ratios necessary to achieve a homogeneous population of ternary αβγ or αβδ receptors. This is of particular importance for investigations aimed at characterizing receptor kinetics and pharmacology, as heterogeneous receptor populations confound analysis. Because αβ receptors are expressed quite efficiently, some groups consider it necessary to transfect the third (*e.g.* γ or δ) subunit in excess, assuming this will ensure a homogeneous ternary receptor population (27, 28). In contrast, other groups have found that equimolar transfection ratios of γ/δ subunit cDNA are sufficient to eliminate the functional signature of α1β2 receptors (1, 29).

Our results demonstrate that γ2L or δ subunit overexpression is unnecessary and likely counterproductive given the aforementioned effects on partnering subunit expression and cell viability. For the γ2 subunit, the flow cytometry and electrophysiology data collectively suggested that the α1β2 receptor population was eliminated early in the cDNA titrations, likely by an α:β:γ subunit cDNA transfection ratio of 1:1:0.3. Of note, many of the kinetic and pharmacological properties of α1β2 receptors were eliminated at even lower γ2 subunit transfection ratios, likely reflecting 7-fold higher charge transfer of α1β2γ2 receptors that obscures the functional signature of α1β2 receptors. For the δ subunit, the results were more dramatic, with the α1β2 receptor population appearing eliminated by α:β:δ subunit cDNA transfection ratio of only 1:1:0.03, reflecting the much higher stability of the δ subunit. It should be emphasized, however, that eliminating the α1β2 receptor population does not guarantee formation of homogeneous receptor populations. The results of the flow cytometry experiments suggest that receptor heterogeneity is already present with α1 and β2 subunit co-expression (Fig. 11, *left column*). Addition of γ2 or δ subunits likely converts this to yet another heterogeneous receptor population (Fig. 11, *middle column*). In other words, receptor heterogeneity may be more of the rule rather than the exception. Although these findings could be artifactual related to heterologous expression, work with under- and overexpressing GABA$_A$ receptor subunit epilepsy-associated mutations further support the idea that native receptor combinations may include a continuum of $\alpha1_2\beta x_3$-$\alpha1_2\beta x_2\gamma2_1$-$\alpha1_2\beta2_1\gamma2_2$ stoichiometries (51).

Interestingly, the electrophysiology titration experiments appear to have reconciled a long-standing debate in the GABA$_A$ receptor literature. Although we have consistently observed αβγ receptor currents that desensitize extensively (52), others have reported poorly desensitizing αβγ receptor currents (53). Notably, different experimental conditions were employed in these experiments, with highly desensitizing currents having been obtained with equimolar transfection ratios, and poorly desensitizing currents having been obtained in the setting of γ2 subunit overexpression. The results from this study indicate that αβγ receptors can have different functional properties depending on the amount of γ2 subunit cDNA transfected, reflecting alterations in receptor stoichiometry. Low levels of γ2 subunit expression yield single γ2 subunit-containing receptors that undergo extensive desensitization, whereas high levels of γ2 subunit expression yield double-γ2 subunit-containing receptors that yield less desensitizing currents (Figs. 9 and 10). Prior results thus likely appeared contradictory because currents were effectively being recorded from different receptor populations.

Although not explicitly verified using concatameric constructs, our electrophysiology results suggest that αβδ receptors also have altered kinetic properties at higher transfection ratios (Fig. 8). Given the similarities between the expression patterns of αβγ and αβδ receptors, the functional changes observed presumably also reflect altered αβδ receptor subunit composition, with receptors formed at the highest transfection ratios likely containing two δ subunits.

Experimental Procedures

Cell Culture and Expression of Recombinant GABA$_A$ Receptors—Human GABA$_A$ receptor α1 (NM_000806), β2 (NM_000813), γ2S (NM_000816), γ2L (NM_198904), and δ (NM_000815) subunits were individually subcloned into the pcDNA3.1+ mammalian expression vector (Invitrogen). Because of the lack of a highly specific, commercially available

antibody targeting an extracellular domain on the γ2 and δ subunits, the HA (YPYDVPDYA) epitope was inserted between amino acids 5 and 6 of the mature δ subunit and between amino acids 4 and 5 of the α1, β2, and γ2 subunits. This resulted in N-terminal sequences of MNDIG**YPYDVPDYA**DYVGS and QKSD**YPYDVPDYA**ADDYED for the mature δ and γ2 subunits, respectively, based on nucleotide sequencing and SignalP predictions. The predicted signal-mature peptide cleavage site was not altered by the HA sequence insertion (data not shown). This insertion site was selected for its known minimal effect on receptor expression and function (24). Although we did not directly evaluate the effect of inserting the HA epitope on γ2 and δ subunit stability, we inferred that stability of these tagged constructs was similar to those of non-tagged subunits given the lack of significant effect on the expression profiles of co-expressed subunits. Specifically, a subset of experiments performed in Figs. 1–3 using HA-tagged γ2 and δ subunits was performed in parallel using non-tagged γ2 and δ subunits, and the profiles of α1 and β2 surface and total cellular expression were found to be nearly identical (data not shown). HA-tagged α1 and β2 constructs were generated for the purposes of FRET experiment in a similar manner, with the HA epitope inserted between amino acids 4 and 5 of the mature peptide. This resulted in an N-terminal sequence of QPSL**YPYDV-PDYA**QDELKDNTTVFT and QSVN**YPYDVPDYA**DPSNM-SLVKE for the mature α1 and β2 subunits, respectively. As with HA-tagged γ2 and δ subunits, HA tagging of the α1 and β2 did not appear to affect expression of partnering subunits (data not shown). Concatenated subunit plasmids were a generous gift from Prof. Erwin Sigel. Synthesis of these constructs has been described previously (6). Briefly, the plasmids contained cDNA from rat α1, β2, and γ2S subunits connected by 10–26 amino acid linkers containing glutamine, alanine, and proline residues. The tandem construct in which the C terminus of the β2 subunit was linked to the N terminus of the α1 subunit will be denoted "β-α" and so forth. The coding region of each vector was sequenced by the Vanderbilt University Medical Center DNA Sequencing Facility and verified against published sequences.

HEK293T cells (American Type Culture Collection, Manassas, VA) were maintained at 37 °C in humidified 5% CO_2, 95% air using Dulbecco's modified Eagle's medium (Invitrogen) supplemented with 10% fetal bovine serum (Invitrogen), 100 IU/ml penicillin (Invitrogen), and 100 μg/ml streptomycin (Invitrogen). Cells were plated at a density of ~10^6 cells per 10-cm culture dish (Corning Glassworks, Corning, NY) and passaged every 2–4 days using trypsin/EDTA (Invitrogen). For flow cytometry and electrophysiology experiments, cells were plated at a density of 4×10^5 cells per 6-cm culture dish (Corning Glassworks) and transfected ~24 h later with equal amounts (1 μg/subunit) of subunit cDNA using FuGENE 6 (Roche Diagnostics) per manufacturer's protocol. In conditions where less than 3 μg of subunit cDNA was transfected, empty pcDNA3.1 vector was added such that a total of 3 μg of cDNA was used for each experimental condition (thus, the "mock" transfection condition consisted of 3 μg of empty pcDNA 3.1 vector cDNA). In the subset of experiments using α:β:γ cDNA transfection ratios of 1:1:3 and 1:1:10, an additional 2 and 9 μg of γ2 subunit

cDNA was transfected, bringing the total amount of cDNA transfected to 5 and 12 μg, respectively. Tandem construct transfection levels were adjusted for the size of the plasmid to deliver equimolar amounts of each subunit cDNA. Specifically, for each 1 μg of single-subunit cDNA transfected, 1.4 μg of triple-subunit and 1.2 μg of double-subunit concatamer cDNA was transfected. Finally, an additional 1 μg of pHook-1 cDNA (encoding the cell surface antibody sFv) was included for electrophysiology experiments so that positively transfected cells could be selected ~24 h later by immunomagnetic bead separation, as described previously (25). Following selection, cells were re-plated at low density on 35-mm dishes for electrophysiological recording the following day.

Electrophysiology—Whole cell patch clamp recordings were obtained at room temperature from lifted cells that were maintained during recordings in a bath solution consisting of (in mM) the following: 142 NaCl, 8 KCl, 6 $MgCl_2$, 1 $CaCl_2$, 10 glucose, and 10 HEPES (pH adjusted to 7.4; 325–330 mosM). All chemicals used for solution preparation were purchased from Sigma. Recording pipettes were pulled from thin-walled borosilicate capillary glass (Fisher) on a Sutter P-2000 micropipette electrode puller (Sutter Instruments, San Rafael, CA) and fire-polished with a microforge (Narishige, East Meadow, NY). When filled with a pipette solution consisting of (in mM) 153 KCl, 1 $MgCl_2$, 5 EGTA, 10 HEPES, and 2 MgATP (pH 7.3; and osmolarity 300–310 mosM) and submerged in the bath solution, yielding open tip resistances of ~1.5–2 megohms and a chloride equilibrium potential (E_{Cl}) of ~0 mV. Currents were recorded at a holding potential of −20 mV using an Axopatch 200B amplifier (Molecular Devices, Foster City, CA), low-pass filtered at 2 kHz using a 4-pole Bessel filter, digitized at 10 kHz using the Digidata 1322A (Molecular Devices), and stored off line for analysis. Because αβδ receptor currents tended to be smaller in amplitude, those recordings (Fig. 8) were obtained at a holding potential of −50 mV. GABA was prepared as a stock solution. Working solutions were made on the day of the experiment by diluting stock solutions with the bath solution.

Analysis of Current Kinetic Properties—For those cells with small (<50 pA) currents, rise time, desensitization, and deactivation were not determined. Analysis of very small currents (usually <10 pA) were determined to be significantly different from zero using a one-sample *t* test. To minimize series resistance error, we recorded current amplitudes from all cells, but we only analyzed the kinetic properties of currents recorded from cells with peak currents less than 6 nA. This cutoff allowed us to minimize the holding voltage error to 1–2 mV (26). Current amplitudes and 10–90% rise times were measured using the Clampfit 9 software package (Molecular Devices). The desensitization and deactivation time courses of $GABA_A$ receptor currents were fit using the Levenberg-Marquardt least squares method with up to four component exponential functions of the form shown in Equation 1,

$$\sum a_n e^{(-t/\tau_n)} + C \qquad \text{(Eq. 1)}$$

where t is time; n is the best number of exponential components; a_n is the relative amplitude of the nth component; τ_n is the time constant of the nth component; and C is the residual

current at the end of the GABA application. The individual time constants fell naturally into four distinct groups ($\tau1 < 16$ ms, $\tau2$ 17–125 ms, $\tau3$ 126–800 ms, and $\tau4 > 800$ ms). The first two time constants (τ_1 and τ_2) were considered to define "fast desensitization." Additional components were accepted only if they significantly improved the fit, as determined by an *F*-test automatically performed by the analysis software on the sum of squared residuals. The time course of deactivation was summarized as a weighted time constant, defined by Equation 2,

$$\frac{\sum a_n \tau_n}{\sum a_n} \qquad \text{(Eq. 2)}$$

Solution exchange time was defined as the time for an open-tip liquid-junction current to increase from 10 to 90% of its maximum value. Data were reported as mean ± S.E. One-way analysis of variance followed by a Dunnett's multiple comparison test was used to compare results to the 1:1:0 and 1:1:1 μg transfection conditions, as indicated.

Flow Cytometry—Cells were harvested ~48 h after transfection using 37 °C trypsin/EDTA (Invitrogen) and placed immediately in 4 °C FACS buffer composed of PBS (Mediatech), 2% fetal bovine serum (FBS) (Invitrogen), and 0.05% sodium azide (VWR Scientific). Cells were then transferred to 96-well plates, where they were washed twice in FACS buffer (*i.e.* pelleted by centrifugation at $450 \times g$, vortexed, and resuspended). For surface protein staining, cells were incubated in antibody-containing FACS buffer for 1 h at 4 °C, washed in FACS buffer three times, and resuspended in 2% w/v paraformaldehyde (Electron Microscopy Sciences). For total protein staining, samples were first fixed and permeabilized using Cytofix/Cytoperm (BD Biosciences) for 15 min. After washing twice with Permwash (BD Biosciences) to remove residual fixative, cells were resuspended in antibody-containing Permwash for 1 h at 4 °C. Following incubation with antibody, samples were washed four times with Permwash and twice with FACS buffer before resuspension in 2% paraformaldehyde. The anti-α1 antibody was obtained from Millipore (clone bd24), conjugated to the Alexa-647 fluorophore using an Invitrogen kit, and used at 4 μg/ml for surface subunit staining and 2 μg/ml for total subunit staining. The anti-β2 antibody was obtained from Millipore (clone 62-3G1) and used at 8 μg/ml for surface subunit staining and 4 μg/ml for total subunit staining. Because anti-β2 antibody conjugation proved inefficient, an anti-IgG1-Alexa-647 secondary antibody was used at a 1:500 dilution for most experiments. The anti-HA antibody (clone 16B12) was obtained from Covance as an Alexa-647 conjugate and used at a 1:250 dilution for surface subunit staining and a 1:500 dilution for total subunit staining.

Samples were run on an LSR II flow cytometer (BD Biosciences). For each staining condition, 50,000 cells were analyzed. Nonviable cells were excluded from analysis based on forward- and side-scatter profiles, as determined from staining with 7-amino-actinomycin D (Invitrogen). The Alexa-555 fluorophore was excited using a 535-nm laser and detected with a 575/26 bandpass filter. The Alexa-647 fluorophore was excited using a 635-nm laser and detected with a 675/20 bandpass filter. Data were acquired using FACSDiva (BD Biosciences) and analyzed off-line using FlowJo 7.1 (Treestar). To compare surface and total expression levels of $GABA_A$ receptor subunits, the mean fluorescence intensity of mock-transfected cells was subtracted from the mean fluorescence intensity of each positively transfected condition. The remaining fluorescence was then normalized to that of a control condition, yielding a relative fluorescence intensity ("Relative FI"). Statistical significance was determined using a one-sample *t* test using a hypothetical mean of 1 (because data in each condition were normalized to wild-type expression). Data were expressed as mean ± S.E.

For protein degradation experiments, cells were plated at a density of 2×10^5 cells per 3-cm culture dish and transfected as described above, but with a total of 1 μg of cDNA for each experimental condition. Approximately 48 h after transfection, 100 μl of 0.1% cycloheximide (Sigma) was added to culture dishes, which were subsequently returned to the 37 °C incubator for the times indicated in the figure legends. After incubation, cells were harvested, permeabilized, stained, and subjected to flow cytometry as described previously.

Radiolabeling, Immunoprecipitation, and SDS-PAGE—HEK293T cells were plated and transfected with $\gamma2L^{HA}$ or δ^{HA} subunit cDNA as described above. Two days after transfection, the culture medium was replaced with methionine-free medium for 30 min and then replaced with medium containing 150 μCi/ml [^{35}S]methionine, and cells were returned to the incubator. For synthesis studies, plates were removed after 5, 10, 15, or 20 min, immediately placed on ice, and washed with both non-radioactive media and PBS. Membranes were lysed using radioimmunoprecipitation assay buffer (RIPA buffer: 50 mM Tris-HCl, pH 7.4, 1% Triton X-100, 250 mM NaCl, 5 mM EDTA) containing protease inhibitor mixture (Sigma), and insoluble components were removed by centrifugation at $15,000 \times g$ for 20 min. The $\gamma2L^{HA}$ and δ^{HA} subunits were incubated overnight with an anti-HA affinity gel (Sigma) and eluted using 125 μg/ml anti-HA peptide (Sigma). Proteins were separated using SDS-PAGE (10% BisTris gel). The dried gel was exposed to a phosphor screen for 2 days and imaged using a Typhoon phosphorimager (Molecular Dynamics/GE Healthcare). The bands then were quantified using ImageJ. Degradation studies were performed identically except that after addition of radioactive medium the cells were returned to 37 °C for 1–4 or 6 h.

Statistical Analysis—All statistical analyses were performed using GraphPad Prism (version 5.02, La Jolla CA) software. Unless otherwise specified, data are expressed as mean ± S.E., and one-way analysis of variance with Tukey's post hoc test was used to determine whether there were significant differences ($p < 0.05$) among different transfection conditions.

Biogenesis of Synaptic αβγ and Extrasynaptic αβδ Receptors

References

1. Haas, K. F., and Macdonald, R. L. (1999) GABA$_A$ receptor subunit γ2 and δ subtypes confer unique kinetic properties on recombinant GABA$_A$ receptor currents in mouse fibroblasts. *J. Physiol.* **514,** 27–45

2. Farrant, M., and Nusser, Z. (2005) Variations on an inhibitory theme: phasic and tonic activation of GABA$_A$ receptors. *Nat. Rev. Neurosci.* **6,** 215–229

3. Mody, I., and Pearce, R. A. (2004) Diversity of inhibitory neurotransmission through GABA$_A$ receptors. *Trends Neurosci.* **27,** 569–575

4. Saxena, N. C., and Macdonald, R. L. (1994) Assembly of GABA$_A$ receptor subunits: role of the δ subunit. *J. Neurosci.* **14,** 7077–7086

5. Baumann, S. W., Baur, R., and Sigel, E. (2001) Subunit arrangement of γ-aminobutyric acid type A receptors. *J. Biol. Chem.* **276,** 36275–36280

6. Baumann, S. W., Baur, R., and Sigel, E. (2002) Forced subunit assembly in α1β2γ2 GABA$_A$ receptors. Insight into the absolute arrangement. *J. Biol. Chem.* **277,** 46020–46025

7. Tretter, V., Ehya, N., Fuchs, K., and Sieghart, W. (1997) Stoichiometry and assembly of a recombinant GABA$_A$ receptor subtype. *J. Neurosci.* **17,** 2728–2737

8. Barrera, N. P., Betts, J., You, H., Henderson, R. M., Martin, I. L., Dunn, S. M., and Edwardson, J. M. (2008) Atomic force microscopy reveals the stoichiometry and subunit arrangement of the α4β3δ GABA$_A$ receptor. *Mol. Pharmacol.* **73,** 960–967

9. Patel, B., Mortensen, M., and Smart, T. G. (2014) Stoichiometry of δ subunit containing GABA$_A$ receptors. *Br. J. Pharmacol.* **171,** 985–994

10. Feng, H. J., Jounaidi, Y., Haburcak, M., Yang, X., and Forman, S. A. (2014) Etomidate produces similar allosteric modulation in α1β3d and α1β3γ2L GABA$_A$ receptors. *Br. J. Pharmacol.* **171,** 789–798

11. Wagoner, K. R., and Czajkowski, C. (2010) Stoichiometry of expressed α4β2δ γ-aminobutyric acid type A receptors depends on the ratio of subunit cDNA transfected. *J. Biol. Chem.* **285,** 14187–14194

12. Kaur, K. H., Baur, R., and Sigel, E. (2009) Unanticipated structural and functional properties of δ-subunit-containing GABA$_A$ receptors. *J. Biol. Chem.* **284,** 7889–7896

13. Eaton, M. M., Bracamontes, J., Shu, H. J., Li, P., Mennerick, S., Steinbach, J. H., and Akk, G. (2014) γ-Aminobutyric acid type A α4, β2, and δ subunits assemble to produce more than one functionally distinct receptor type. *Mol. Pharmacol.* **86,** 647–656

14. Boileau, A. J., Pearce, R. A., and Czajkowski, C. (2005) Tandem subunits effectively constrain GABA$_A$ receptor stoichiometry and recapitulate receptor kinetics but are insensitive to GABA$_A$ receptor-associated protein. *J. Neurosci.* **25,** 11219–11230

15. Kellenberger, S., Eckenstein, S., Baur, R., Malherbe, P., Buhr, A., and Sigel, E. (1996) Subunit stoichiometry of oligomeric membrane proteins: GABA$_A$ receptors isolated by selective immunoprecipitation from the cell surface. *Neuropharmacology* **35,** 1403–1411

16. Khan, Z. U., Gutierrez, A., and De Blas, A. L. (1994) The subunit composition of a GABA$_A$/benzodiazepine receptor from rat cerebellum. *J. Neurochem.* **63,** 371–374

17. Backus, K. H., Arigoni, M., Drescher, U., Scheurer, L., Malherbe, P., Möhler, H., and Benson, J. A. (1993) Stoichiometry of a recombinant GABA$_A$ receptor deduced from mutation-induced rectification. *Neuroreport* **5,** 285–288

18. Quirk, K., Gillard, N. P., Ragan, C. I., Whiting, P. J., and McKernan, R. M. (1994) Model of subunit composition of γ-aminobutyric acid A receptor subtypes expressed in rat cerebellum with respect to their α and γ/δ subunits. *J. Biol. Chem.* **269,** 16020–16028

19. Khan, Z. U., Gutiérrez, A., and De Blas, A. L. (1994) Short and long form γ2 subunits of the GABA$_A$/benzodiazepine receptors. *J. Neurochem.* **63,** 1466–1476

20. Benke, D., Honer, M., Michel, C., and Mohler, H. (1996) GABA$_A$ receptor subtypes differentiated by their γ-subunit variants: prevalence, pharmacology and subunit architecture. *Neuropharmacology* **35,** 1413–1423

21. Bollan, K. A., Baur, R., Hales, T. G., Sigel, E., and Connolly, C. N. (2008) The promiscuous role of the ε subunit in GABA$_A$ receptor biogenesis. *Mol. Cell. Neurosci.* **37,** 610–621

22. Minier, F., and Sigel, E. (2004) Techniques: Use of concatenated subunits for the study of ligand-gated ion channels. *Trends Pharmacol. Sci.* **25,** 499–503

23. Ericksen, S. S., and Boileau, A. J. (2007) Tandem couture: Cys-loop receptor concatemer insights and caveats. *Mol. Neurobiol.* **35,** 113–128

24. Connolly, C. N., Krishek, B. J., McDonald, B. J., Smart, T. G., and Moss, S. J. (1996) Assembly and cell surface expression of heteromeric and homomeric γ-aminobutyric acid type A receptors. *J. Biol. Chem.* **271,** 89–96

25. Greenfield, L. J., Jr, Sun, F., Neelands, T. R., Burgard, E. C., Donnelly, J. L., and MacDonald, R. L. (1997) Expression of functional GABA$_A$ receptors in transfected L929 cells isolated by immunomagnetic bead separation. *Neuropharmacology* **36,** 63–73

26. Rula, E. Y., Lagrange, A. H., Jacobs, M. M., Hu, N., Macdonald, R. L., and Emeson, R. B. (2008) Developmental modulation of GABA$_A$ receptor function by RNA editing. *J. Neurosci.* **28,** 6196–6201

27. Boileau, A. J., Baur, R., Sharkey, L. M., Sigel, E., and Czajkowski, C. (2002) The relative amount of cRNA coding for γ2 subunits affects stimulation by benzodiazepines in GABA$_A$ receptors expressed in *Xenopus* oocytes. *Neuropharmacology* **43,** 695–700

28. Boileau, A. J., Li, T., Benkwitz, C., Czajkowski, C., and Pearce, R. A. (2003) Effects of γ2S subunit incorporation on GABA$_A$ receptor macroscopic kinetics. *Neuropharmacology* **44,** 1003–1012

29. Angelotti, T. P., and Macdonald, R. L. (1993) Assembly of GABA$_A$ receptor subunits: α1β1 and α1β1γ2S subunits produce unique ion channels with dissimilar single-channel properties. *J. Neurosci.* **13,** 1429–1440

30. Gorrie, G. H., Vallis, Y., Stephenson, A., Whitfield, J., Browning, B., Smart, T. G., and Moss, S. J. (1997) Assembly of GABA$_A$ receptors composed of α1 and β2 subunits in both cultured neurons and fibroblasts. *J. Neurosci.* **17,** 6587–6596

31. Wooltorton, J. R., Moss, S. J., and Smart, T. G. (1997) Pharmacological and physiological characterization of murine homomeric β3 GABA$_A$ receptors. *Eur. J. Neurosci.* **9,** 2225–2235

32. Thomas, P., and Smart, T. G. (2005) HEK293 cell line: a vehicle for the expression of recombinant proteins. *J. Pharmacol. Toxicol. Methods* **51,** 187–200

33. Connolly, C. N., Uren, J. M., Thomas, P., Gorrie, G. H., Gibson, A., Smart, T. G., and Moss, S. J. (1999) Subcellular localization and endocytosis of homomeric γ2 subunit splice variants of γ-aminobutyric acid type A receptors. *Mol. Cell. Neurosci.* **13,** 259–271

34. Olsen, R. W., and Sieghart, W. (2008) International Union of Pharmacology. LXX. Subtypes of γ-aminobutyric acid(A) receptors: classification on the basis of subunit composition, pharmacology, and function. Update. *Pharmacol. Rev.* **60,** 243–260

35. Selvin, P. R. (2000) The renaissance of fluorescence resonance energy transfer. *Nat. Struct. Biol.* **7,** 730–734

36. Shrestha, D., Jenei, A., Nagy, P., Vereb, G., and **Szöllősi,** J. (2015) Understanding FRET as a research tool for cellular studies. *Int. J. Mol. Sci.* **16,** 6718–6756

37. Ernst, M., Bruckner, S., Boresch, S., and Sieghart, W. (2005) Comparative models of GABA$_A$ receptor extracellular and transmembrane domains: important insights in pharmacology and function. *Mol. Pharmacol.* **68,** 1291–1300

38. Miller, P. S., and Aricescu, A. R. (2014) Crystal structure of a human GABA$_A$ receptor. *Nature* **512,** 270–275

39. Zhao, J., Matthies, D. S., Botzolakis, E. J., Macdonald, R. L., Blakely, R. D., and Hedera, P. (2008) Hereditary spastic paraplegia-associated mutations in the NIPA1 gene and its *Caenorhabditis elegans* homolog trigger neural degeneration *in vitro* and *in vivo* through a gain-of-function mechanism. *J. Neurosci.* **28,** 13938–13951

40. Kozak, M. (1986) Point mutations define a sequence flanking the AUG initiator codon that modulates translation by eukaryotic ribosomes. *Cell* **44,** 283–292

41. Kang, J. Q., Shen, W., Lee, M., Gallagher, M. J., and Macdonald, R. L. (2010) Slow degradation and aggregation *in vitro* of mutant GABA$_A$ re-

ceptor γ2(Q351X) subunits associated with epilepsy. *J. Neurosci.* **30,** 13895–13905

42. Hosie, A. M., Dunne, E. L., Harvey, R. J., and Smart, T. G. (2003) Zinc-mediated inhibition of GABA_A receptors: discrete binding sites underlie subtype specificity. *Nat. Neurosci.* **6,** 362–369

43. Günther, U., Benson, J., Benke, D., Fritschy, J. M., Reyes, G., Knoflach, F., Crestani, F., Aguzzi, A., Arigoni, M., and Lang, Y. (1995) Benzodiazepine-insensitive mice generated by targeted disruption of the γ2 subunit gene of γ-aminobutyric acid type A receptors. *Proc. Natl. Acad. Sci. U.S.A.* **92,** 7749–7753

44. Hanson, S. M., and Czajkowski, C. (2008) Structural mechanisms underlying benzodiazepine modulation of the GABA_A receptor. *J. Neurosci.* **28,** 3490–3499

45. Taylor, P. M., Thomas, P., Gorrie, G. H., Connolly, C. N., Smart, T. G., and Moss, S. J. (1999) Identification of amino acid residues within GABA_A receptor β subunits that mediate both homomeric and heteromeric receptor expression. *J. Neurosci.* **19,** 6360–6371

46. Hackam, A. S., Wang, T. L., Guggino, W. B., and Cutting, G. R. (1997) A 100 amino acid region in the GABA ρ1 subunit confers robust homo-oligomeric expression. *Neuroreport* **8,** 1425–1430

47. Bracamontes, J. R., and Steinbach, J. H. (2008) Multiple modes for conferring surface expression of homomeric β1 GABA_A receptors. *J. Biol. Chem.* **283,** 26128–26136

48. Boileau, A. J., Pearce, R. A., and Czajkowski, C. (2010) The short splice variant of the γ2 subunit acts as an external modulator of GABA_A receptor function. *J. Neurosci.* **30,** 4895–4903

49. Baumann, S. W., Baur, R., and Sigel, E. (2003) Individual properties of the two functional agonist sites in GABA_A receptors. *J. Neurosci.* **23,** 11158–11166

50. Sigel, E., and Barnard, E. A. (1984) A γ-aminobutyric acid/benzodiazepine receptor complex from bovine cerebral cortex. Improved purification with preservation of regulatory sites and their interactions. *J. Biol. Chem.* **259,** 7219–7223

51. Johnston, A. J., Kang, J. Q., Shen, W., Pickrell, W. O., Cushion, T. D., Davies, J. S., Baer, K., Mullins, J. G., Hammond, C. L., Chung, S. K., Thomas, R. H., White, C., Smith, P. E., Macdonald, R. L., and Rees, M. I. (2014) A novel GABRG2 mutation, p.R136*, in a family with GEFS+ and extended phenotypes. *Neurobiol. Dis.* **64,** 131–141

52. Bianchi, M. T., Song, L., Zhang, H., and Macdonald, R. L. (2002) Two different mechanisms of disinhibition produced by GABA_A receptor mutations linked to epilepsy in humans. *J. Neurosci.* **22,** 5321–5327

53. Bowser, D. N., Wagner, D. A., Czajkowski, C., Cromer, B. A., Parker, M. W., Wallace, R. H., Harkin, L. A., Mulley, J. C., Marini, C., Berkovic, S. F., Williams, D. A., Jones, M. V., and Petrou, S. (2002) Altered kinetics and benzodiazepine sensitivity of a GABA_A receptor subunit mutation [γ2(R43Q)] found in human epilepsy. *Proc. Natl. Acad. Sci. U.S.A.* **99,** 15170–15175